ISSN 0429-8284

Whole Number 229

e-Front runners

FUJI ELECTRIC REVIEW

2

2010 VOL.56

Power Semiconductor contributing in energy and environment region

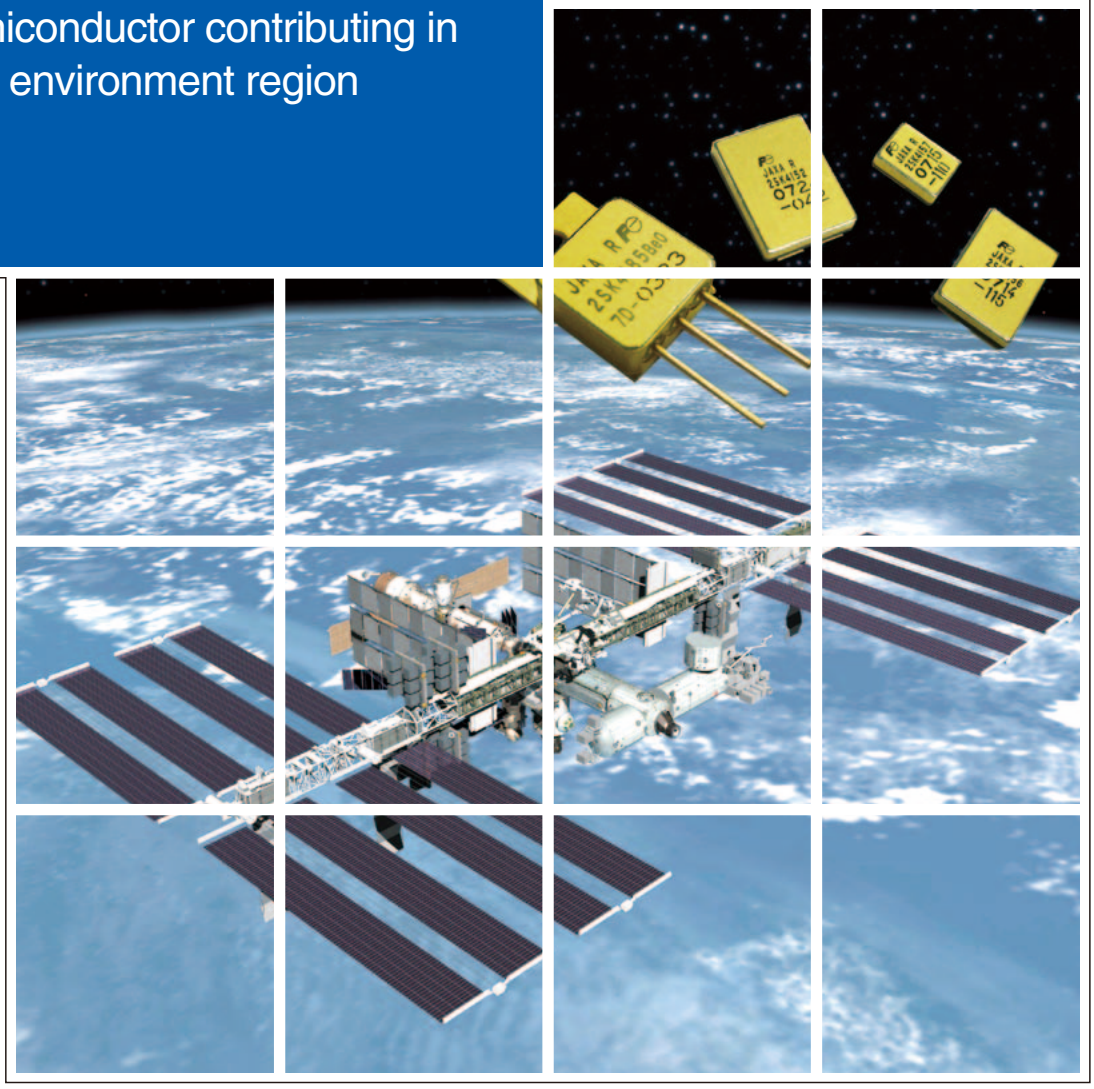

Fuji Electric Group

e-Front runners

The seeds of energy

The responsibility for protecting the global environment and leaving a secure future for subsequent generations is ours.
Photovoltaic power generation, wind power generation, hybrid cars, electric cars ...
Fuji Electric Systems contributes to the realization of more effective energy utilization and greater energy savings in all fields with high-efficiency, high-precision, and compact and lightweight packages. A creative and abundant future will sprout from these “seeds of energy.” Fuji Electric’s power semiconductors.

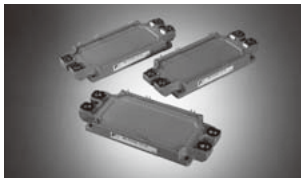
IGBT modules

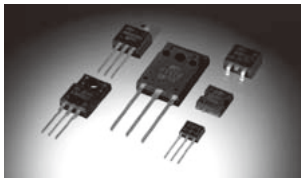
Power MOSFETs

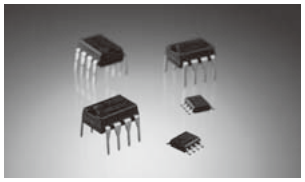
Power ICs

Fuji Electric Systems Co., Ltd.

Gate City Ohsaki, East Tower, 1-11-2 Osaki, Shinagawa-ku, Tokyo 141-0032, JAPAN TEL.03-5435-7114 www.fujielectric.com/fes/

FUJI ELECTRIC
REVIEW

2
2010 VOL.56

Power Semiconductor contributing
in energy and environment region

CONTENTS

The Current Status and Future Outlook for Power Semiconductors 47

3.3 kV IGBT Modules 51

New Lineup of V-Series IGBT Modules 56

V-Series Intelligent Power Modules 60

Superjunction MOSFET 65

High Reliability Power MOSFETs for Space Applications 69

Pressure Sensor for Exhaust Systems 74

Thermal Management Technology for IGBT Modules 79

Cover photo:

To protect the earth from global warming, there are many things that mankind must do. While harnessing the synergistic effect from power electronics and power semiconductors to boost the power of each, Fuji Electric is focusing on the "energy" and "environment" fields, and is working to make energy more environmentally-friendly and to help conserve the global environment.

Fuji Electric's power semiconductors are also used in outer space, where higher reliability and greater energy savings are required than on land.

The cover image shows Fuji Electric's space-use high-reliability MOSFETs (Metal-Oxide-Semiconductor Field-Effect Transistors) that are being used in the International Space Station. Fuji Electric's power semiconductors help to achieve energy savings not only on the Space station, but also on Spaceship Earth, and where they are making a positive contribution to protecting the environment.

FUJI ELECTRIC REVIEW vol.56 no.2 2010
date of issue: May 20, 2010

editor-in-chief and publisher Hisao Shigekane
Corporate R & D Headquarters
Fuji Electric Holdings Co., Ltd.
Gate City Ohsaki, East Tower,
11-2, Osaki 1-chome, Shinagawa-ku,
Tokyo 141-0032, Japan
http://www.fujielectric.co.jp

editorial office Fuji Electric Journal Editorial Office
c/o Fuji Office & Life Service Co., Ltd.
9-4, Asahigaoka 1-chome, Hino-shi, Tokyo 191-0065, Japan

The Current Status and Future Outlook for Power Semiconductors

Yasukazu Seki † **Toru Hosen** † **Masaru Yamazoe** ‡

ABSTRACT

With the increased focus on efforts to protect the global environment, power semiconductors, which are the main power electronics products, are becoming increasingly important. Using 6th-generation IGBT V-Series technology, Fuji Electric has developed and commercialized high voltage, large capacity power modules that are capable of operating at high temperatures. As post-silicon technology for the next generation, we are pursuing the development of devices that utilize wide band gap semiconductor material and the development of superjunction MOSFETs. Additionally, MOSFETs designed for applications in outer space and used in the Japanese experimental module known as "Kibo" attain high reliability and low loss, while ICs designed for use in power supply control achieve low noise and energy savings. Exhaust system pressure sensors for use in automobiles and control ICs for use in hybrid vehicles have been newly commercialized.

1. Introduction

In 2009, the Obama administration established and inaugurated the Green New Deal. In September of the same year, at the United Nations Summit on Climate Change, Japanese Prime Minister Hatoyama announced a new mid-term goal of cutting Japan's greenhouse gas emissions by 25% from 1990 levels by 2020. Among the new policies set forth by leaders from the various countries, projects related to energy and environment attracted the most attention.

Fuji Electric is presently reforming its business structure to focus on "energy and the environment." Also, Fuji Electric has long been involved in efforts to develop innovative power electronics technology which is crucial for protecting the global environment and reducing CO_2 emissions. Power electronics technology is a key technology for converting energy into power, and as the main components, power semiconductors are becoming more and more important.

The performance characteristics requested of power semiconductors are low loss, high speed switching, low noise and ease of use.

This paper discusses the current status and future outlook for the energy-saving and environmentally-friendly power semiconductors which are being developed by Fuji Electric and their representative products of power modules, power discretes, power supply ICs and automotive devices.

2. Power Modules

With a commitment to energy savings and eco-friendliness, IGBT (insulated gate bipolar transistor) power modules are being deployed in various fields. The IGBT chip at the core of these modules is a 6th generation IGBT chip, which has begun to be deployed in Fuji Electric's "V-Series." As can be seen in Fig. 1, many items are requested of the IGBT modules but a tradeoff relation exists between the requested items and performance characteristics, and numerous technological breakthroughs would be needed to satisfy all the requests.

Fig.1 Requested characteristics of IGBT modules

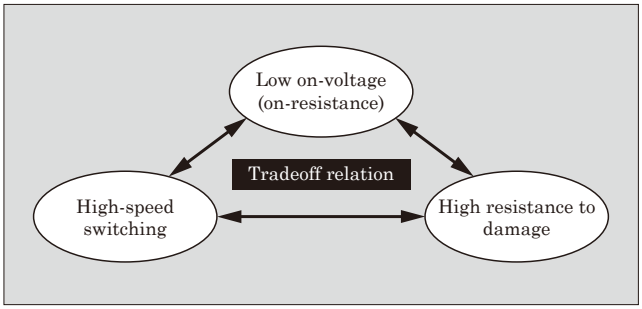

With the "V-Series" 6th generation IGBT module, the attained characteristics are close to their theoretical limits and dissipation loss was reduced. Also, the design was implemented with good awareness of the environment. For example, the "V-Series" complies with the RoHS directive*1 through the use of lead-free materials, the package structure significantly reduces generated noise, and a small size and light weight are realized simultaneously. Additionally, high temperature operation up to 175 °C is possible.

A series of 600 V, 1,200 V and 1,700 V IGBT modules and IPMs have been commercialized using these

† Semiconductors Group, Fuji Electric Systems Co., Ltd.
‡ Fuji Electric Systems Co., Ltd.

*1: RoHS: EU Directive on the restriction of the use of certain hazardous substances in electrical and electronic equipment

superior V-Series IGBTs.

Fuji Electric has previously developed IGBT modules and IPMs (intelligent power modules) for use in hybrid vehicles. As key components for hybrid vehicles, Fuji Electric has also previously developed plated IGBT and FWD (free wheeling diode) chips housed in a package having a double-sided cooling structure. This IGBT achieves approximately twice the current density of a general-purpose IGBT. Now, with the additional application of 6th generation IGBT V-Series technology and microfabrication technology, and by improving the FS (field stop) structure, a dramatic improvement in characteristics has been achieved. Moreover, temperature sensing and current sensing functions have been built-in to realize a chip that is even easier to use.

As an example application to the energy and environment field, high-voltage high-power IGBT modules have begun to be used in wind power generators. As a result of recent trends of applications involving wind power generation, there is strong demand for high-voltage and high-power IGBT modules, and in response, Fuji Electric has prepared 1,200 V, 1,700 V and 3,300 V high-power modules. A wide variety of standard package groups including the HPM (high power module), EconoPACK+ and the like, have been assembled and are being deployed by our customers.

As new types of IGBTs, the RB-IGBT (reverse blocking IGBT) and RC-IGBT (reverse conduction IGBT) are being developed by Fuji Electric. In particular, as next-generation applications for the RB-IGBT, application to the highly-anticipated matrix converters and application to a new 3-level inverter are promising.

3. Next Generation Power Modules

The characteristics of the 6th generation IGBT V-Series are approaching the theoretical limits of silicon. Silicon carbide (SiC) and gallium nitride (GaN) are the leading candidates for materials to be used instead of silicon in next-generation power devices. Due to material properties well suited for use in power devices, research and development of SiC material has been ongoing for a long time, and recently, practical applications have begun to be considered. SiC material is very expensive due to the difficulty of growing its crystals and the process technology involved, but a way toward a technical solution is gradually becoming visible, and sooner or later the cost issue is also expected to be resolved.

Moreover, GaN, which became prominent with blue diodes, has also been found to be a promising material for power devices, and is a candidate for the material used in next-generation power devices. Despite having only a short history of use as a power device material, the decisive factor for GaN, which can be fabricated on a silicon wafer, will be whether or not the advantage of its inexpensive cost can be leveraged.

Both SiC and GaN are promising candidates as the material of future power devices. Fuji Electric and the National Institute of Advanced Industrial Science and Technology (AIST) are conducting joint research of SiC material. Also, Fuji Electric and Furukawa Electric Co., Ltd. have jointly established a next-generation power device technical research association to research GaN, and plan to incorporate the results into the next-generation power modules.

4. Power Discretes

As a high-voltage MOSFET (Metal-Oxide-Semiconductor Field-Effect-Transistor), Fuji Electric has newly developed the "Superjunction MOSFET" (SJ-MOSFET). In 2008, Fuji Electric developed the "SuperFAP-E^{3S} 600 V Series" having the industry's lowest level of $R_{on} \cdot A$ (on-resistance normalized to a unit area) as a planer MOSFET, which realized low noise and an improved tradeoff relation between low loss and switching performance, and contributed to higher efficiency in devices. Recently, in the field of switching power supplies, which is the main application of MOSFETs, efforts to realize higher efficiency have been accelerated in order to comply with international energy-saving regulations such as the International Energy Star Program. In particular, a power supply efficiency of 92% or above (at 50% load) is requested of the large-capacity servers and the like used at internet data centers, which are essential for IT companies. To realize this high efficiency, MOSFETs must also have lower loss characteristics, and therefore Fuji Electric developed the new low on-resistance SJ-MOSFET. The SJ-MOSFET has the industry's lowest level of $R_{on} \cdot A$, and realizes approximately 1/4th the on-resistance of the previous "SuperFAP-E^{3S} Series." When installed in the power factor improvement circuit of a power supply, as shown in Fig. 2, loss is reduced by approximately 14% and development is accelerating toward the goal of early product commercialization.

Fig.2 Comparison of power MOSFET dissipation loss (input AC100 V/output 400 W)

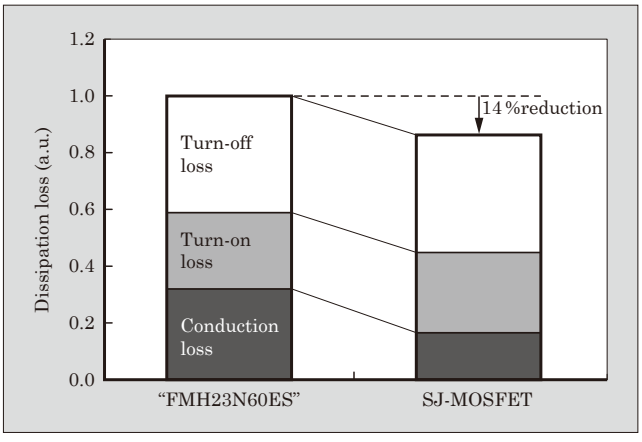

Fuji Electric has also commercialized highly reliable MOSFETs for space applications such as in artificial satellites. In 1994, Fuji Electric's initial space-use devices were installed in and contributed to the successful launch of the first rocket built exclusively in Japan. Leveraging that experience and incorporating subsequent research and development results, the present lineup of space-use MOSFETs overcame prior obstacles to achieve low on-resistance and the required tolerance to ionization radiation and high-energy charged particles in outer space. Additionally, these MOSFETs are installed in "Kibo," the Japanese Experimental Module of the International Space Station, and have continued to operate properly since being launched into orbit in 2008. In the future, Fuji Electric intends to expand the range of applications to overseas space industries as well.

Meanwhile, Fuji Electric has developed a Schottky barrier diode (SBD) having an ultra low I_R and suitable for use in a high temperature environment such as for photovoltaic power generation. The reverse leakage current I_R has been reduced to 1/10th that of a conventional SBD, enabling guaranteed operation at junction temperatures of up to 175 °C.

Through joint development with third parties, as described above, Fuji Electric is accelerating the development of next-generation devices that use SiC and GaN to realize dramatically lower loss compared to the present generation of silicon-based devices.

5. Power Supply Control ICs

To help achieve energy savings and lower noise in switching power supplies and to lower the cost of devices, Fuji Electric has independently developed and applied a control method for power supply control ICs. Devices such as televisions, PCs and printers that are plugged-in continuously an electrical outlet remain in a standby state for extended periods of time. Their consumption of power during standby must be reduced in order to save energy. The EPA 5.0 standard issued by the U.S. Environmental Protection Agency prescribes the average efficiency even during light-load operation, and in response, Fuji Electric developed the "FA5592 Series" of current mode PWM control ICs that comply with the EPA 5.0 standard. The FA5592 significantly improves efficiency during light load operation, as shown in Fig. 3, by reducing the switching frequency when the load rate is below 60%. Moreover, with a built-in switching frequency distribution function that realizes lower noise and an internal startup circuit that ensures operation at up to 750 V, the FA5592 can be used in countries or regions in which there are large fluctuations in power supply voltage.

For relatively large-capacity power supplies, "FA5604/FA5605" multifunction voltage mode PMW control ICs and "FA5610/FA5611" low-noise continuous current mode PFC control ICs have been developed, and realize both high performance and small size in a SOP8 pin package. In particular, the FA5610N realizes a high power factor and low noise with an oscillation frequency distribution function, enabling the input filter to be simplified.

Fig.3 Dependence of power supply efficiency on load current for FA5592

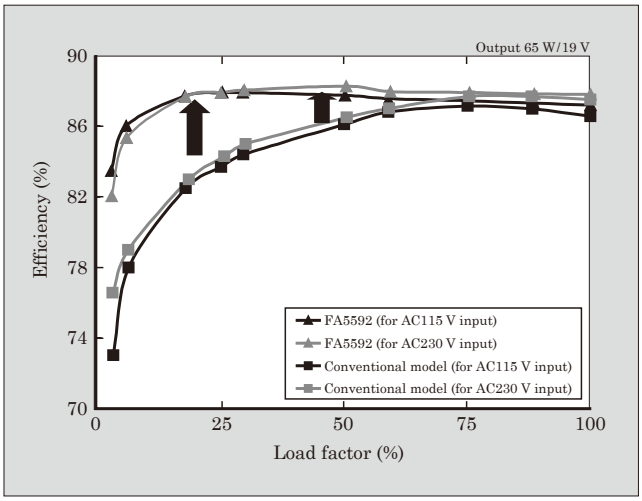

In the power supply control IC field, to satisfy increasingly severe requirements for higher efficiency, energy savings, smaller size, lower device cost and the like, Fuji Electric continues to research and develop a distinctive, proprietary control method.

6. Automotive Devices

As automotive devices, IPSs (intelligent power switches), exhaust system pressure sensors, and the "Fi009" hybrid vehicle IGBT drive IC have been developed by Fuji Electric.

(1) Exhaust system sensor

Automotive exhaust gas regulations are becoming more stringent year after year, and in 2009, the Post New Long-term Regulations in Japan and the Euro 5 emissions standards in Europe came into force. As a result, exhaust gas recirculation systems, in which a portion of exhaust gas is recirculated to the intake side so as to control combustion in an engine, have begun to be used. Newly developed exhaust system pressure sensors, based on the CMOS (Complementary Metal-Oxide-Semiconductor) single-chip technology that has been applied to conventional intake system pressure sensors, utilize a new structure to realize dramatically improved corrosion resistance. On the basis of this technology, product development continues with the aim of application to heavy machinery and the like.

(2) Fi009 driving IC for hybrid vehicle IGBTs

The demand for highly fuel-efficient hybrid vehicles, which are provided with both a gasoline engine and an electric motor so as to optimize load-sharing according to the running conditions of the automobile, is increasing rapidly. IGBTs are the main devices used

in the inverter systems that drive the motor in hybrid vehicles. The control IC that drives this IGBT has the important function of protecting the IGBT in order to ensure high reliability of the inverter system. The newly developed control IC has a function that protects against overheating and overcurrent, and receives signals from temperature and current sensors inside the IGBT chip made by Fuji Electric.

In addition to the products introduced herein, Fuji Electric's automotive devices also include single-chip igniters and other products that use Fuji Electric's proprietary and distinctive technology. Leveraging this technology, Fuji Electric intends to continue to develop highly reliable and high performance products that satisfy customer needs.

7. Postscript

With protection of the global environment being an important topic of today, the implementation of environmental measures such as reducing CO_2 emissions and the development of new energy sources that do not depend on fossil fuels are urgently needed. With a commitment to energy savings and eco-friendliness, Fuji Electric is actively addressing these problems and aims to contribute their solutions. For this purpose, technical innovation in power semiconductors, the key components of power electronics technology, is absolutely necessary.

As has been discussed in this paper, Fuji Electric is working to develop distinctive power semiconductor products, and will apply innovative technology to realize lower loss, more advanced functionality, smaller size, higher reliability and lower noise. Fuji Electric intends to continue to advance technical development with the aim of developing products from the customer's perspective.

3.3 kV IGBT Modules

Takeharu Koga † Yasuhiko Arita † Takatoshi Kobayashi †

ABSTRACT

Fuji Electric has developed a 3.3 kV-1.2 kA IGBT module in response to market needs for inverters suitable for industrial and vehicle applications. The package of the newly developed module incorporates IGBT high-power module technology. Compared to previous modules, internal inductance has been reduced by 33% and the current flow to chips on each insulating substrates shows good uniformity. Power cycle tests were implemented with this module, and sufficient durability was verified. 3.3 kV-0.8 kA IGBT modules has been developed. 3.3 kV-1.5 kA and 3.3 kV-0.8 kA IGBT modules are also being developed to expand the product lineup.

1. Introduction

IGBT (Insulated Gate Bipolar Transistor) modules have gained widespread popularity due to their low loss characteristics, suitability for configuring simple driving circuits, wide safety operation area and high reliability. The high-voltage high-power sector in which GTO (Gate Turn-OFF) thyristors have been used widely is also transitioning to the use of IGBT modules. IGBT modules are being applied widely in high power inverter and high voltage inverter systems and the like. Especially as a result of recent efforts to prevent global warming, the market for new energy (wind power generation, solar power generation) has grown rapidly. The inverter systems used in this sector have been advanced to achieve higher power capacities, and demand for IGBT modules is growing.

Fuji Electric has previously developed high-power IGBT modules for application to the high-power sector. In 2007, Fuji Electric enhanced the chip, package design and manufacturing technology of the previous high-power 1.2 kV and 1.7 kV IGBT modules to develop a 3.3 kV 1.2 A high-power IGBT module. In 2008, Fuji Electric improved the low-loss, thermal characteristics and environmental durability of the 1.2 kV and 1.7 kV modules to develop new high-power IGBT modules[(1)] and is expanding its product lineup. The package of these modules has low inductance and achieves excellent current balance.

This package technology is also applied to the newly developed 3.3 kV 1.2 kA IGBT module. The 3.3 kV IGBT modules are designed for use in vehicle applications as well as industrial applications. This paper presents an overview and describes the performance of the new 3.3 kV IGBT modules.

† Semiconductors Group, Fuji Electric Systems Co., Ltd.

2. Specifications of 3.3 kV IGBT Module

Figure 1 shows an external view of 3.3 kV 12 kA IGBT module. With a package size of 190 mm × 140 mm, the module is compatible with modules made by other companies. Table 1 lists the target specifications of the 3.3 kV modules.

3. Electrical Characteristics

3.1 IGBT and FWD characteristics

(1) IGBT chip characteristics

IGBT chips incorporate a trench structure and a field stop (FS) structure (U-Series IGBT) that provide an excellent trade-off in the relation between the collector-emitter saturation voltage $V_{CE(sat)}$ and turn-off loss Eoff, and utilize a cell-pitch optimized for 3.3 kV to achieve lower loss. Also, in the high-power sector, it is essential that an IGBT chip has high-power switching capability (wide reverse bias safety operation area (RBSOA) and short-circuit capability) in order to realize high reliability. To provide a wide RBSOA, the

Fig.1 External view of 3.3 kV 1.2 kA IGBT module

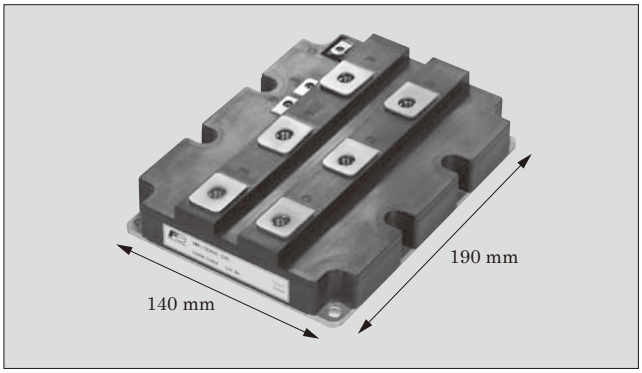

Table 1 Target specifications of 3.3 kV IGBT module (1.5 kA modules are under development)

Item		Symbol	1MBI1200UE-330	1MBI1500UE-330	1MBI800UG-330	Units
Collector current		I_C	1,200	1,500	800	A
Package size		—	190×140	190×140	130×140	mm
Collector-Emitter saturation voltage (chip)		$V_{CE(sat)}$	3.15 V (typical value) (at 150 °C and 1,200 A)	3.15 V (typical value) (at 150 °C and 1,500A)	3.15 V (typical value) (at 150 °C and 800 A)	V
Forward voltage (chip)		V_F	2.75 V (typical value) (at 150 °C and 1,200 A)	2.75 V (typical value) (at 150 °C and 1,500 A)	2.75 V (typical value) (at 150 °C and 800 A)	V
Thermal resistance	IGBT	$R_{th(j-c)}$	8.5	8.0	13.0	K/kW
	FWD		17.0	15.0	25.0	K/kW
Isolation voltage		V_{iso}	6.0	6.0	6.0	kV

Fig.2 $V_{CE(sat)}$-I_C characteristics

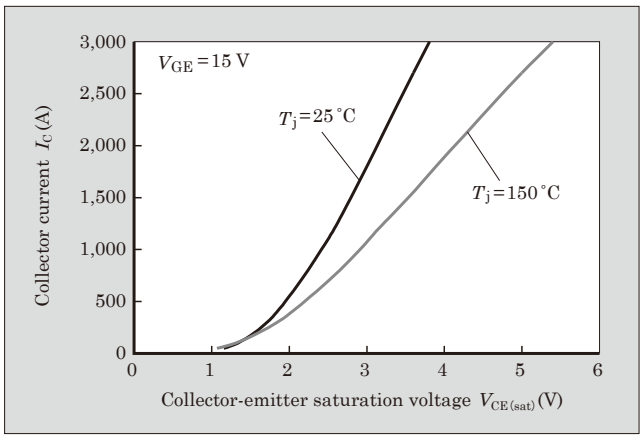

Fig.3 V_F-I_F characteristics

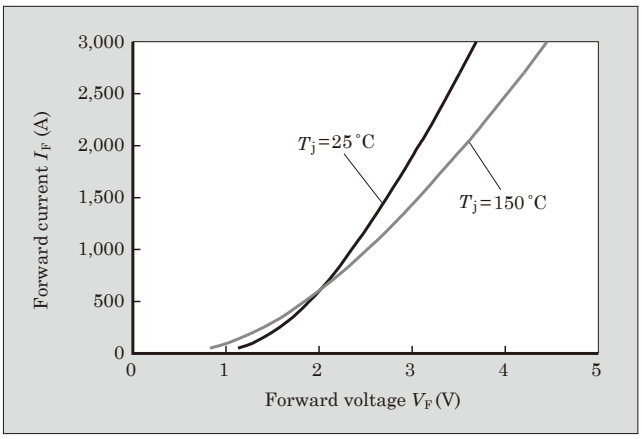

chip was designed with a structure that suppresses the concentration of current at the edge of the active area. In addition, carrier injection on the collector side is adjusted to ensure sufficient short-circuit capability.

(2) FWD (Free Wheeling Diode) chip characteristics

In order to achieve (1) lower loss and (2) suppression of oscillation and surge voltage during reverse recovery at low current levels, FWD chips are designed with an optimized crystalline wafer structure and a deep collector-side n^+ layer concentration profile. Also, to provide high reverse recovery capability (high di/dt capability) the cathode-side is designed with a structure that suppresses the concentration of current at the edge of the active area.

3.2 $V_{CE(sat)}$-I_C characteristics and V_F-I_F characteristics

Figure 2 shows the $V_{CE(sat)}$-I_C characteristics. Similar to Fuji Electric's low-voltage class of trench IGBTs, a positive temperature coefficient is exhibited. With a reduced current imbalance for parallel connections, these modules allows for easy parallel connections necessary for achieving larger currents.

Figure 3 shows the V_F-I_F characteristics. The FWD, at a forward voltage, also exhibits a positive temperature coefficient at currents of at least one-half of the rated value, and allows for easy parallel connections.

Fig.4 Switching waveforms (inductive load) (V_{CC}=1,800 V, I_C=1,200 A, T_j=150 °C)

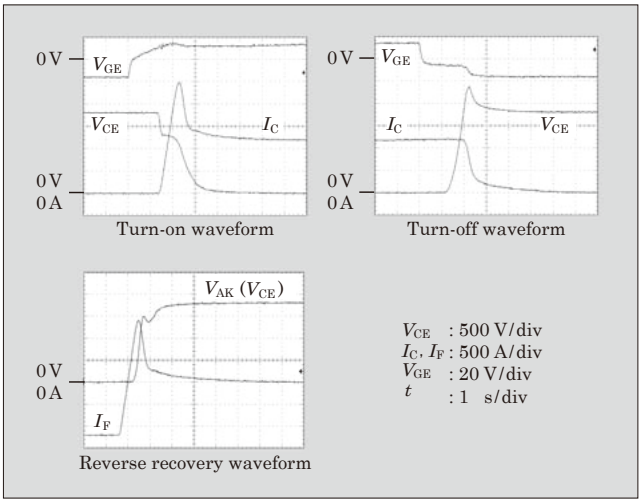

3.3 Switching characteristics

Figure 4 shows the turn-on, turn-off and reverse recovery waveforms. These waveforms, exhibiting neither noise nor the generation of a large surge voltage, are free of problems.

4. Package Structure

High reliability and high thermal conductivity (low thermal resistance) are required for the high-power

modules used in high-power inverter system. The reduction of current imbalances among chips inside a module and the reduction of heat generation in a package are also important issues for achieving large currents.

4.1 General internal structure of package

Figure 5 shows the general internal structure of a 3.3 kV IGBT module.

To enhance the heat dissipation capability of the insulating substrate in a 3.3 kV module, instead of the alumina and silicon nitride substrates typically used with low-voltage modules, an AlN substrate having 2.5 to 8 times the thermal conductivity was used. The result realized the low thermal resistance shown in Table 1.

A copper (Cu) base is typically used as the base material in low-voltage modules. With the 3.3 kV IGBT modules, an AlSiC base is used to ensure high reliability. AlSiC is a composite of Al and SiC, and because its coefficient of thermal expansion is close to that of the AlN substrate, the heat cycle lifetime and power cycle lifetime are several times higher than in the case of a Cu base.

4.2 Improved structure of main terminal

In the design of the main terminal, the following three items are very important.

(a) Reduction of internal inductance
(b) Reduction of current imbalance of chips on each insulating substrates
(c) Reduction of stress at contact areas with insulating substrates (leading to higher heat cycle and power cycle lifetimes)

Fig.5 General internal structure of 3.3 kV IGBT module

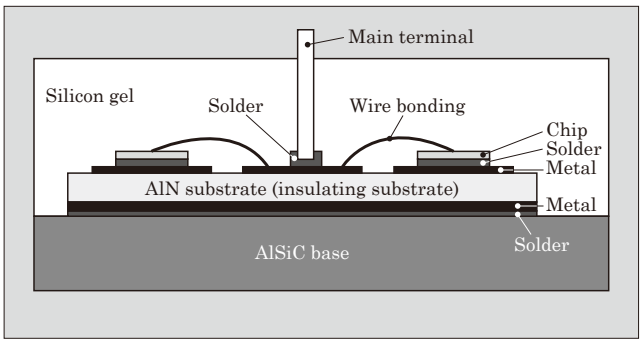

Fig.6 Main terminal before and after improvement

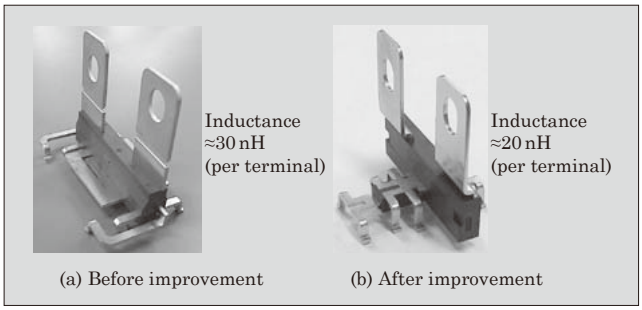

The main terminal was changed to the same new structure as used with high-power IGBT modules. Figure 6 shows the main terminal before and after the improvement.

(1) Reduction of internal inductance

The internal inductance was reduced by shortening the length of the main terminal lead as much as possible, arranging the conducting areas of the collector and the emitter leads vertically, and by actively using the mutual interaction of the magnetic field.

Measured results show that the internal inductance has been reduced from 30 nH for a conventional terminal to 20 nH. According to the value of the internal inductance L and the current turn $\mathrm{d}i/\mathrm{d}t$ during switching, a voltage $\Delta V = L \cdot (\mathrm{d}i/\mathrm{d}t)$ is generated between the chip and the contact area of the terminal. Therefore a reduction in internal inductance reduces the overvoltage applied to the chip.

(2) Reduction of current imbalance between insulating substrates

Because of the main terminal arrangement of the module, the insulating substrate is separated into a substrate directly below the emitter terminal and a substrate directly below the collector terminal. These are connected in parallel with the shortest possible lead, thereby forming a structure in which a current imbalance between insulating substrates occurs easily.

Fig.7 Measured current distribution of chips on each insulating substrates

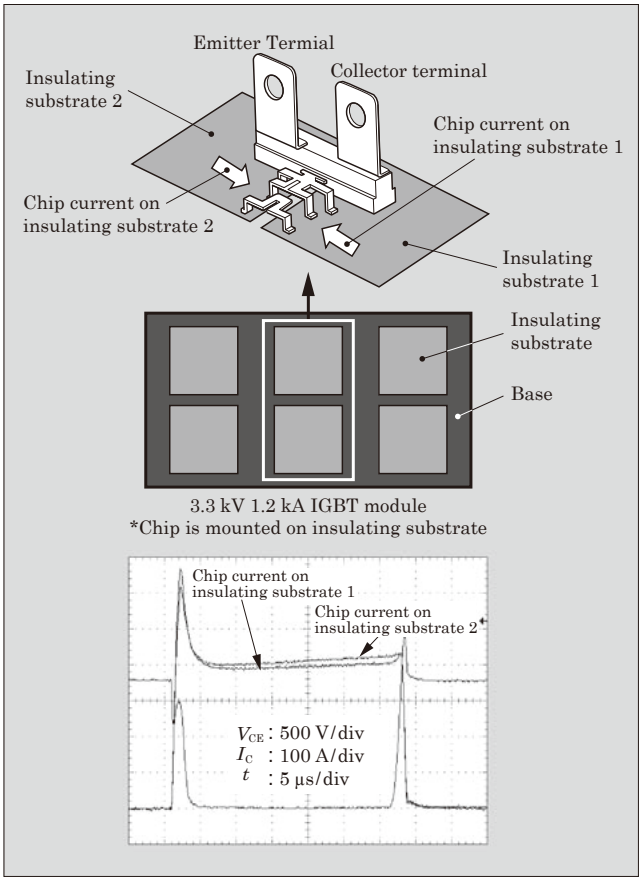

Fig.8 ΔT_j power cycle test results

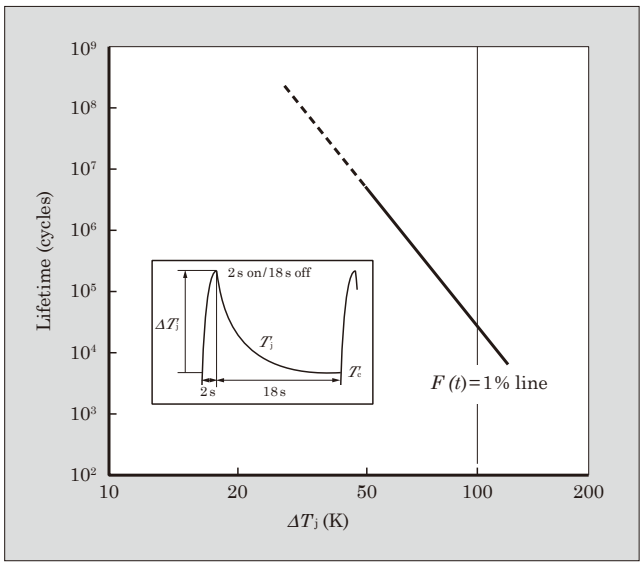

Fig.9 ΔT_c power cycle test results

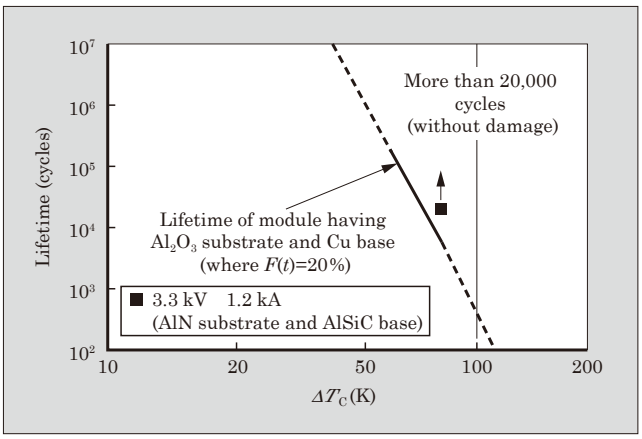

The path of current flow in the emitter terminal and the collector terminal were analyzed. The structure was designed such that the currents would be equal.

Figure 7 shows waveforms of the current distribution measured of chips on each insulating substrates. The measured results and the distribution of current of chips on each insulating substrates were good.

(3) Reduction of stress at contact areas with insulating substrate

To reduce the stress at contact areas with the insulating substrate, an optimized heat treatment is applied to soften the material of the main terminal. Also, the main terminal is integrally formed with the terminal case so as to lessen the generation of stress on the main terminal.

5. Ensuring Power Cycle Capability

High-voltage modules are required to provide high reliability for their intended applications. In the marketplace, the reliability considered to be important is the power cycle capability. A power cycle test (intermittent power-on test) is performed by applying energized and isolated electrical loads to an IGBT module with its heat dissipating fin temperature held constant, and causing the junction temperature T_j of the IGBT chip to rise and fall so as to generate thermal stress, and the test is carried out until the thermal stress damages the chip. Types of power cycle tests include the ΔT_j power cycle test that causes the junction temperature to rise and fall with a relatively short period and the ΔT_c power cycle test that causes the case temperature T_c to rise up and fall to a certain temperature with a long period.

5.1 ΔT_j power cycle evaluation results

From module analysis performed after a power cycle test of an IGBT module, Fuji Electric has verified that the ΔT_j power cycle capability is determined by the lifespan of the solder underneath the chip and aluminum wire junction of the chip.

Figure 8 shows the ΔT_j power cycle test results for 3.3 kV modules. The 3.3 kV modules, as in the case of the 1.2 kV and 1.7 kV high-power IGBT modules, use highly rigid Sn-Ag solder underneath the chip. By equalizing the current of chips on each the insulating substrates, ΔT_j power cycle test results that are equivalent to those of the 1.2 kV and 1.7 kV high-power IGBT modules could be verified.

5.2 ΔT_c power cycle test results

As shown in Fig. 9, a power cycle capability of more than 20,000 cycles was verified under the condition of ΔT_c=80 K. The 3.3 kV modules use an AlSiC base and thus have at least 3 times the ΔT_c power cycle capability as in the case of a copper base.

6. Product Lineup

At present, a 3.3 kV 1.5 kA IGBT module having the same package size as the 3.3 kV 1.2 kA IGBT (190 mm × 140 mm) but with larger IGBT and FWD chip sizees are being developed. A 3.3 kV 800 A IGBT module having a 130 mm × 140 m package size has been developed. The target specifications for each 3.3 kV IGBT module are listed in Table 1.

7. Postscript

Fuji Electric has recently developed a 3.3 kV 1.2 kA IGBT module as a high-power IGBT module in a package. Compared to the module characteristics prior to improvement, internal inductance has been reduced by 33% and the current flow of chips on each insulating substrates showed good uniformity. Power cycle tests were carried out with this module and sufficient durability was verified. 3.3 kV 1.2 kA IGBT module is planned for commercial release in 2010.

References

(1) Nishimura, T. et al. High-power IGBT Modules. Fuji Electric Review. 2008, vol.55, no.2, p.51-55.

(2) Morozumi, A. et al. Reliability of Power Cycling for IGBT Power Semiconductor Module. Conf. Rec. IEEE Ind. Appl. Conf. 36th. 2001, p.1912-1918.

New Lineup of V-Series IGBT Modules

Kouta Takahashi † **Shinichi Yoshiwatari** † **Yusuke Sekino** †

ABSTRACT

Fuji Electric is developing a series of products that use the latest generation "V-Series" IGBTs. V-Series IGBT modules realize lower chip loss and improved package heat dissipation to achieve a smaller IGBT module size and higher power density. The chip and package characteristics have also been improved to enhance reliability and guarantee the maximum temperature of 175˚C. For these high power density and highly reliable V-Series IGBTs, Fuji Electric has developed new packages, such as a large capacity 2-in-1 package and a small sized PIM (Power Integrated Module) package. The product lineup will be expanded up to 1,700 V.

1. Introduction

Energy savings and the reduction of CO_2 emissions have been seen as important challenges for the industrial sector in recent years. As a result, the demand for inverters is continuing to increase. In consideration of power dissipation, switching capability, drive circuit design and the like, the power semiconductors used most commonly in inverters are IGBTs (insulated gate bipolar transistors).

Fuji Electric developed a line of commercial IGBTs in 1988, and since then has responded to market needs by steadily releasing successive generations of new models that realize low loss and a compact size. Recently, Fuji Electric has realized even lower levels of loss and a more compact size with its lineup of "V-Series" IGBT modules that incorporate the latest generation of IGBTs. Also, the V-Series of IGBT modules feature enhanced chip and package characteristics that improve reliability and enable the guarantee of (non-continuous) operation at chip junction temperatures of T_j=175 °C when the inverter is in an emergency operation.

This paper discusses the reliability and product lineup of Fuji Electric's V-Series of IGBT modules.

2. IGBT V-Series Characteristics[1]

Figure 1 shows the changes in chip size for successive generations of the IGBT chips installed in commercially available IGBT modules. Fuji Electric has reduced the chip size by 50% over 10 years, and the V-Series further shrinks the die size by an additional 30% compared to the U-Series. With the V-Series, the use of a silicon nitride substrate (SiN) having good thermal conductivity as the insulating substrate, in addition to chip improvements, improves the heat dissipation performance and increases the power density of the IGBT module. These improvements contribute significantly to reducing the size and lowering the cost of the entire inverter system. Also, with the V-Series, the optimization of the MOS (metal-oxide-semiconductor) gate structure facilitates control of the abrupt behavior of the IGBT current and FWD (free-wheeling diode) voltage during turn-on switching, which is a cause of EM (electromagnetic) noise[2]. Accordingly, the V-Series of IGBT modules facilitate EM noise reduction and inverter design.

3. Reliability of V-Series of IGBT Modules

Not only are the V-Series of IGBT modules compact in size and have good noise controllability, but they are also highly reliable. With the V-Series, non-continuous operation is guaranteed during instantaneous emergency operation at temperatures of up to

Fig.1 Reduction of IGBT chip size

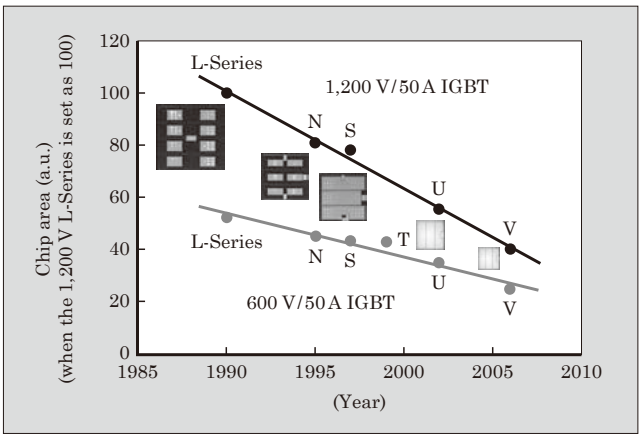

† Semiconductors Group, Fuji Electric Systems Co., Ltd.

175 °C, and continuous operation is guaranteed during normal operation conditions at temperatures of up to 150 °C. Compared to the U-Series, this is an increase of 25 °C for each operating state. To make this possible, Fuji Electric improved the reliability and switching capability of the IGBT chip during high-temperature operation, and also improved the package reliability, including the solder and Al bond wires. Details of these accomplishments are described below.

To guarantee operation during instantaneous emergency conditions at temperatures of up to 175 °C, reverse blocking capacity must be maintained even at high temperatures and the chip must be capable of stable switching even at large currents. We have verified that with the V-Series, an IGBT with no lifetime killer and a FWD that uses electron irradiation as carrier lifetime control enables a stable breakdown voltage to be maintained, without thermal runaway, at temperatures of up to 200 °C. Also, to verify the high-temperature switching capability, we have verified IGBT switching and FWD switching at 200 °C. Figure 2 shows IGBT turn-off waveforms for a chip junction temperature T_j=200 °C at twice the rated current. Based on these results, the V-Series is able to guarantee operation during instantaneous emergency conditions at temperatures of up to 175 °C.

To guarantee during normal operation at temperatures of up to 150 °C, long-term reliability of the chip's breakdown voltage, and reliability of the package, including solder and wire bonding, are essential. The long-term reliability of a chip's breakdown voltage is usually verified with an accelerated aging test in which a DC voltage is applied to a chip while being heated

Fig.2 High-temperature switching waveform of 1,200 V "V-Series" IGBT

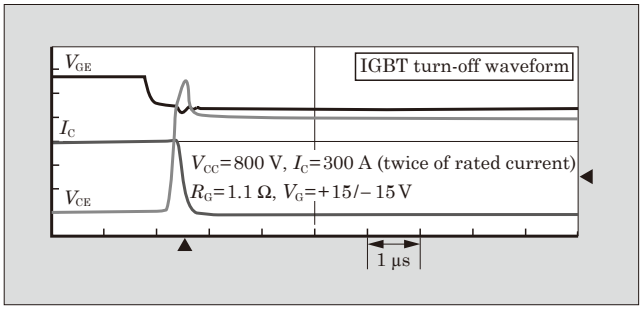

Fig.3 Breakdown voltage reliability test results for 1,200 V "V-Series" FWD

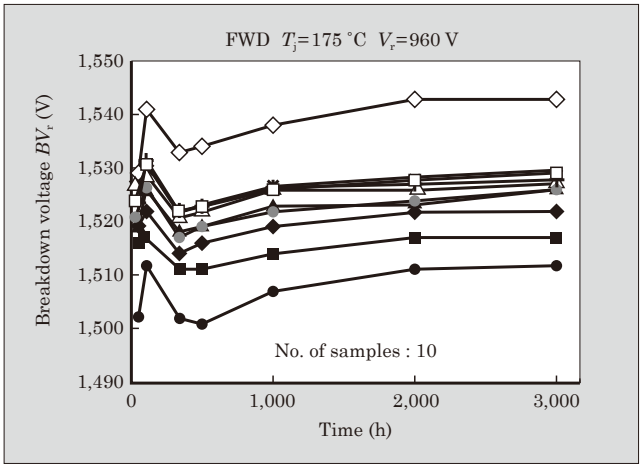

Fig.4 1,200 V "V-Series" power cycle test results

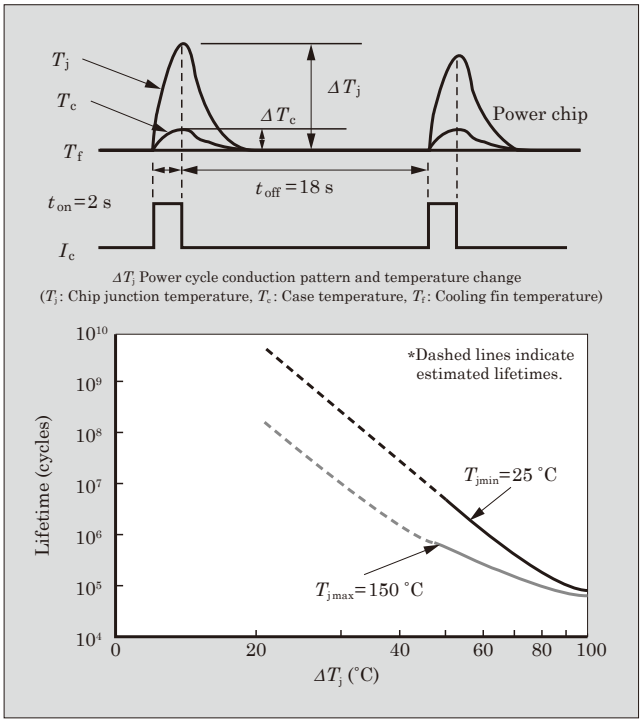

Fig.5 1,200 V "V-Series" PIM series and New Dual series

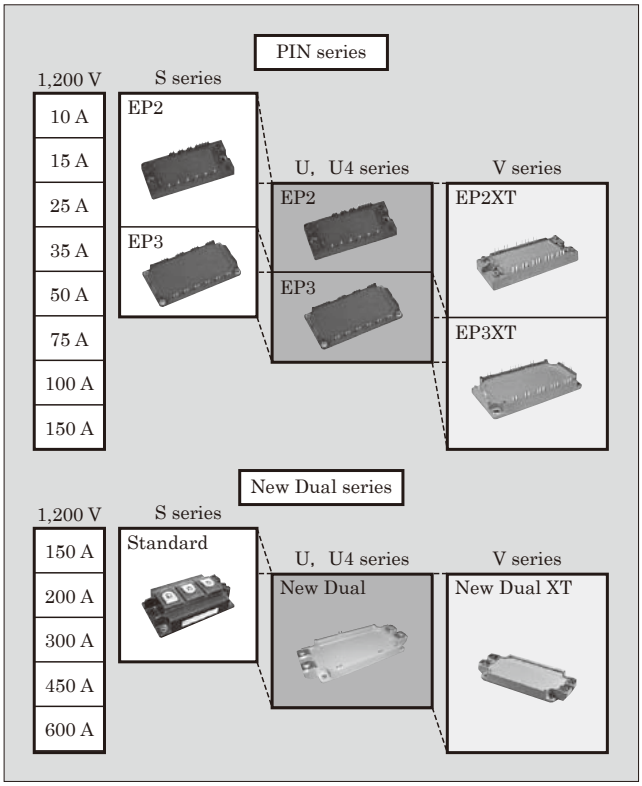

Fig.6 Future expansion of the “V-Series” lineup

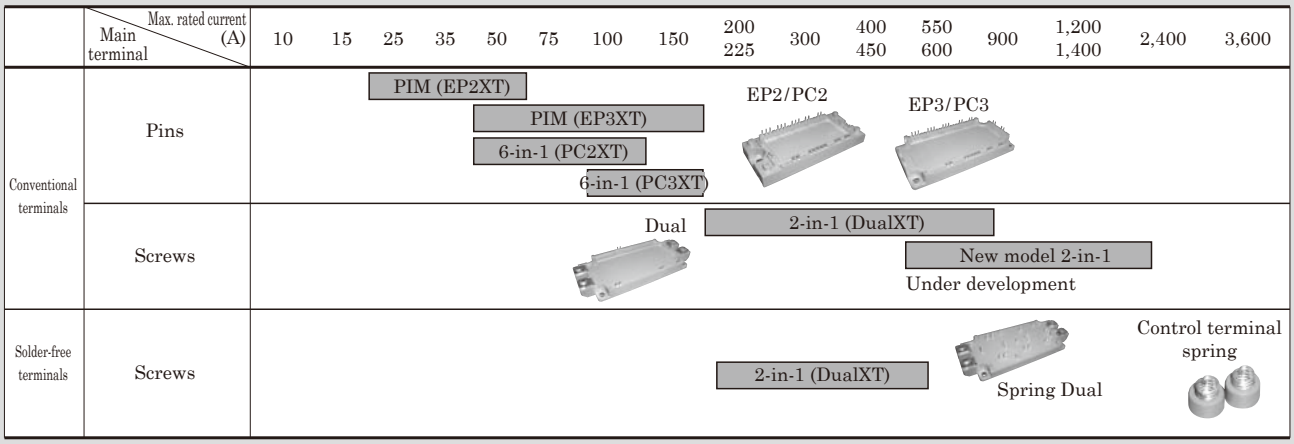

(a) 1,200 V series

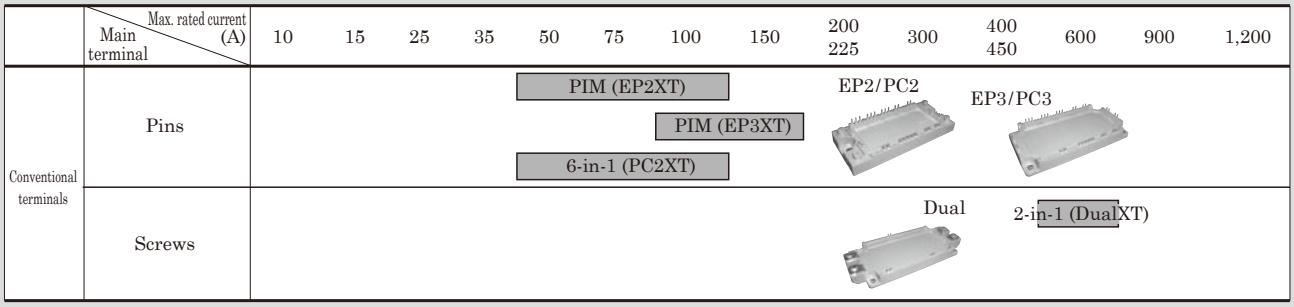

(b) 600 V series

in an electronic oven. Figure 3 shows the results of a FWD reliability test. For a T_j (chip temperature) of 175 °C, we verified that sufficient reliability is exhibited, without degradation of the breakdown voltage, even after 80% of the rated voltage had been applied for 3,000 hours. An IGBT having a similar junction termination as the FWD was found to have the equivalent reliability.

Typically, in a power module, the package reliability is affected by repeated thermal cycles, wherein a chip becomes hot while in the on-state and then becomes cool during the off-state, and as a result, the solder and wire bonding contact underneath the chip are stressed by thermal expansion and contraction. Sufficient capacity to withstand this stress is necessary. Figure 4 shows the results of a V-Series power cycle test. The T_{jmin}=25 °C line indicates the chip's lifetime (number of cycles) when the cooling fin temperature is held constant and the maximum chip junction temperature is varied during the load cycle. For example, ΔT_j=30 °C represents a load cycle in which the cooling fin temperature is 25 °C and the maximum chip temperature is 55 °C. The T_{jmax}=150 °C line indicates the chip's lifetime when the maximum chip temperature is held constant and the cooling fin temperature is varied during the load cycle. For example, when ΔT_j=30 °C, the cooling fin temperature is 125 °C and the maximum chip temperature is 150 °C during the load cycle.

As shown in the graph, even if ΔT_j is the same, higher cooling fin and chip temperatures result in shorter lifetimes. In other words, the T_{jmax}=150 °C line represents the worst case operating conditions, but even under these conditions, it was still possible to verify that the V-Series provides sufficient reliability with a lifetime of more than 50,000 cycles at ΔT_j=100 °C. Based on these results, the improvements to the chip and package reliability guarantee the normal operation of the V-Series at temperatures of up to 150 °C.

Thus, the reliability of the V-Series during high-temperature operation has been improved significantly, and this improved reliability contributes greatly to enhancing the inverter reliability and the degree of freedom in the thermal design.

4. Lineup of V-Series IGBT Modules

At present, the V-Series is available in PIM (power integrated module) and New Dual models as shown in Fig. 5.

The PIM models integrate upper and lower arm IGBTs and FWDs for 3 phases, a converter diode and a brake IGBT (7-in-1), enabling a 3-phase AC inverter to be configured from a single module. As a result, an

inverter system can be made more compact in size and the design can be streamlined. For the V-Series, the lineup of PIM models was expanded up to a rated current of 150 A.

The New Dual models are provided for use with rated currents of 200 A and above. These modules integrate upper and lower arm IGBTs and FWDs for 1 phase (2-in-1). Three chips are used in parallel inside the module. When power semiconductors are used in parallel, there is a concern that a current imbalance will occur in which current is concentrated in some chips. The New Dual models feature an innovative internal interconnect pattern that results in an extremely easy-to-use device with almost no current imbalance among chips. For the V-Series, the lineup of New Dual models was expanded up to a rated current of 600 A.

5. Future Outlook

Fuji Electric plans to continue to expand the V-Series lineup. Future plans for expansion of the lineup are shown in Fig. 6. Development of the following new packages is being advanced.

(1) High-power modules (Econo PACK+*1, new 2-in-1)
(2) Compact module (MiniSKiiP*2)

Presently, the market for high-power inverters for electric power transformer applications such as wind power generators, traction applications and the like is expanding, and Fuji Electric plans to develop high-power modules to meet the needs of these markets. We plan to develop a line of EconoPACK+ models up to rated values of 550 A and 1,200 V, and a new 2-in-1 model up to rated values of 1,400 A and 1,200 V. Also, for low-power applications, Fuji Electric is developing the MiniSKiip, which is solder-free, is easy to assemble and has equivalent functions as the PIM models but with a significantly smaller size. We plan to develop a line of MiniSKiip models rated at 8 to 100 A and 1,200 V.

Additionally, Fuji Electric is also developing a 1,700 V chip, and plans to deploy this chip in successive high-power applications such as the new 2-in-1 and New Dual models.

*1: Econo PACK is a trademark or registered trademark of Infineon Technologies AG.
*2: MiniSKiiP is a trademark or a registered trademark of SEMIKRON.

6. Postscript

This paper has described the features and lineup of Fuji Electric's "V-Series" IGBT modules that use the latest generation IGBT chips. Through improved chip technology and package heat dissipation performance, the V-Series achieves a smaller size and will significantly aid in the production of more compact inverters. Moreover, improved reliability of the chip and package enables the operation to be guaranteed at temperatures up to 175 °C. Consequently, the V-Series makes an important contribution to enhancing the inverter reliability and the degree of freedom in the thermal design.

In the future, Fuji Electric plans to deploy the V-Series technology in 1,700 V high-power modules and compact modules, and will to continue to support the needs of our customers.

References

(1) Onozawa, Y., et al. "U-Series IGBT Modules (1,200 V)," Fuji Electric Journal. 2002, vol.75, no.10, p.563-566.
(2) Igarashi, S., et al. "Analysis and Reduction Methods of EMI Radiation Noise from Converter Systems," IEEJ Transactions on Industry Applications. 1998, vol.118-D, no.6, p.757-766. (Japanese).

V-Series Intelligent Power Modules

Naoki Shimizu † Hideaki Takahashi † Keishirou Kumada †

ABSTRACT

Fuji Electric has developed a series of intelligent power modules for industrial applications, known as V-Series IPMs. This product combines high-performance 6th-generation V-chip technology for the IPMs with a new control IC to realize lower loss and a smaller package size. The short-circuit protection function was made to operate at faster speeds and the trade-off relation between conduction loss and short-circuit withstand capability was improved to reduce switching loss. Additionally, the new control IC and the package were optimized to reduce turn-on loss and improve radiation noise characteristics. In addition to the conventional protection functions, a new function that outputs different alarm pulse widths for each alarm factor is also provided. Ground-fault protection can also be provided even in a small package.

1. Introduction

An IPM (Intelligent Power Module) is an intelligent power device that combines a standard IGBT module containing an IGBT (Insulated Gate Bipolar Transistor) chip and a FWD (Free Wheeling Diode) with a drive IC equipped with drive and protective functions. IPMs are used in machines in a wide range of fields, but mostly in motor-driven equipment (such as NC (Numerical Control) machine tools, general-purpose inverters, servos, air conditioners and elevators) and power supply devices (such as UPS (Uninterruptible Power Supplies), and PCS (Power Conditioning Systems) for solar energy generation), and are required to have compact size, high efficiency, low noise, long life and high reliability.

Fuji Electric, in 1997, devised the industry's first internal IGBT chip over-temperature protection function, and developed the "R-IPM Series" that aimed to achieve higher reliability with an all-silicon design that reduced the number of parts. In 2002, Fuji Electric developed the "R-IPM3 Series" in which the chip structure was changed from PT (punch through) to NPT (non-punch through). In 2004, Fuji Electric integrated a newly developed NPT-type trench-gate structure IGBT and a new structure FWD into the "U-IPM Series" which improves the tradeoff relation between lower switching loss and radiation noise.

Recently, Fuji Electric has developed an FS (field stop) type "V-Series" IGBT chip (V-IGBT) having a trench gate structure that achieves even lower loss and lower input capacitance. Fuji Electric has also developed a drive IC that uses finer line widths to realize a more compact size, and features improved temperature characteristics with less variation among chips. These technologies and packages have been optimized to develop the "V-Series IPM" (V-IPM) that is housed in a new compact package and that features an improved tradeoff relation between total dissipation loss and radiation noise. This paper describes Fuji Electric's new V-IPMs.

2. Product Concept and Product Lineup

Development concepts for the V-IPM are listed below.

(1) Reduction of total dissipation loss
(2) Improvement of tradeoff relation between switching loss and radiation noise
(3) Shorter dead time
(4) Individual outputs for each cause of alarm
(5) More compact and thinner packages
(6) Provision of ground fault protection for small capacity packages
(7) Compliance with RoHS*1 directive

Details of these concepts are explained in chapters 3 to 6 below.

Table 1 shows the V-IPM product lineup. For V-IPM devices, the current capacity has been increased compared to the previous devices, and 600 V-rated devices have rated currents of 20 to 400 A, and 1,200 V-rated devices have rated currents of 10 to 200 A. The four types of newly developed packages are all RoHS compliant.

Table 2 lists characteristics and internal functions of the V-IPM devices. A small capacity package (P629) newly realizes short-circuit protection (ground fault protection) function in its upper arm. Also, throughout

† Semiconductors Group, Fuji Electric Systems Co., Ltd.

*1: RoHS: EU Directive on the restriction of the use of certain hazardous substances in electrical and electronic equipment

Table 1 V-IPM product lineup

(a) Product lineup

Rated voltage	Number of elements	20 A	30 A	50 A	75 A	100 A	150 A	200 A	300 A	400 A
600 V	6 in 1	P629*								
				P626						
	6 in 1 7 in 1			P630*						
								P631*		

Rated voltage	Number of elements	10 A	15 A	25 A	35 A	50 A	75 A	100 A	150 A	200 A
1,200 V	6 in 1	P629*								
				P626						
	6 in 1 7 in 1			P630*						
								P631*		

* : Upgrade of capacity compared to existing products

(b) Package types

P629 package	P626 package	P630 package	P631 package
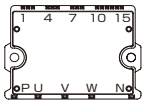	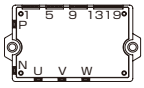	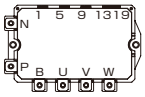	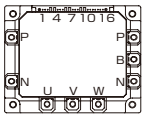
L×W×H (mm)	L×W×H (mm)	L×W×H (mm)	L×W×H (mm)
49.5×70×12	50×87×12	84×128.5×14	110×142×27

Table 2 V-IPM characteristics and internal functions

Package	Arm	Drive circuit	Over current protection	Short-circuit protection	Chip over temperature protection	Low voltage protection	Alarm output
P629	Upper	○	○	◎	○	○	–
	Lower	○	○	○	○	○	◎
P626	Upper	○	○	○	○	○	◎
	Lower	○	○	○	○	○	◎
P630	Upper	○	○	○	○	○	◎
	Lower	○	○	○	○	○	◎
P631	Upper	○	○	○	○	○	◎
	Lower	○	○	○	○	○	◎

◎ : Improvement from existing product

the lineup, a pulse output width that changes according to the alarm cause makes it possible to specify the cause of the alarm.

3. Characteristics of V-IPM Power Chips

V-Series IPMs are utilizing 6 th generation V-IGBT chips. The V-IGBT is an FS-type IGBT having a trench gate structure formed by using thin wafer process technology with a FZ (floating zone) wafer. Figure 1 compares the cross-sectional structure of various chips, and Table 3 shows the history of IGBT technology.

The surface structure has been optimized to make

Fig.1 Comparison of IGBT chip cross-sectional structures (660 V-IPM)

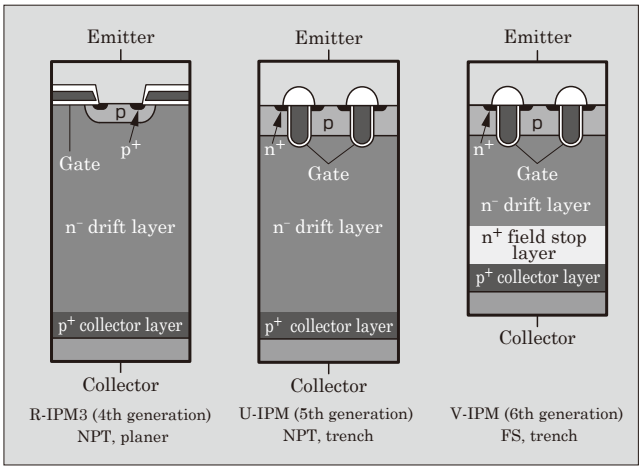

Table 3 History of IGBT technology (600 V-IPM)

IGBT technology	Generation	3rd generation	4rd generation	5rd generation	6rd generation
	IPM	R-IPM	R-IPM3	U-IPM	V-IPM
	IGBT	N-IGBT	T-IGBT	U-IGBT	V-IGBT

Wafer	Epitaxial	FZ	
Structure	PT	NPT	FS
Gate structure	Planar	Trench	
Lifetime control	Yes	No	
Carrier injection	High injection	Low injection	
Transport efficiency	Low efficiency	High efficiency	

a drift layer have lower resistance and be thinner. As the result, the V-IGBT has the advantage of lower on-voltage $V_{CE(sat)}$ and improved switching loss. Additionally, the optimization of the surface structure and the lower resistance of the drift layer also improve the controllability of the turn-on di/dt. The radiation noise is less than compared to a conventional device.

The IGBT chip for the V-IPM, compared to a chip for an IGBT module, realizes an improved tradeoff relation between $V_{CE(sat)}$ and turn-off loss E_{off} as a result of a finer surface structure. When $V_{CE(sat)}$ is reduced, the short-circuit current increases and the short-circuit withstand capability decreases, and short-circuit protection must engage rapidly in practical applications.

The FWD with improved lifetime control realizes lower recovery current and soft recovery.

4. Characteristics

4.1 Total dissipation loss

The marketplace requests IPMs to have lower loss. There are two objectives for reducing the loss, one is to increase the carrier frequency in order to improve equipment controllability, and the other is to increase the output current at the same carrier frequency.

Also, the reduction in loss will lead to reduced cost of the equipment since less cooling capability will be required than before.

Figure 2 compares examples of dissipation loss during PWM inverter operation. The loss in the V-IPM is approximately 27% lower than that of the R-IPM, approximately 17% lower than that of the R-IPM3, and approximately 10% lower than that of the U-IPM.

This reduction in loss is due to an improved tradeoff relation between $V_{CE(sat)}$ and E_{off}, and a lower turn-on loss E_{on}. These techniques for reducing loss are described below.

4.2 Improvement of $V_{CE(sat)}$ and E_{off} tradeoff relation

Static loss and E_{off} account for more than 50% of the total loss in an IGBT chip. However, as shown in Fig. 3, tradeoff relations exist among $V_{CE(sat)}$, which determines the static loss of the IGBT chip, E_{off} and the short-circuit withstand capability, This tradeoff must be optimized. Since the IPM has a short-circuit protection function, by increasing the speed of the short-circuit protection, the IGBT chip short-circuit withstand capability can be diverted to reduce loss. With the V-IPM, the achievement of higher speed short-circuit protection resulted in an improved tradeoff relation between $V_{CE(sat)}$ and E_{off}, and lower loss.

Fig.2 Comparison of total dissipation loss (simulation results)

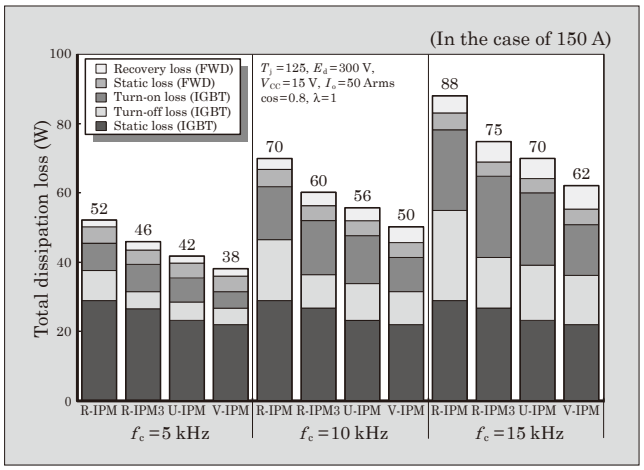

Fig.3 IGBT tradeoff relationships

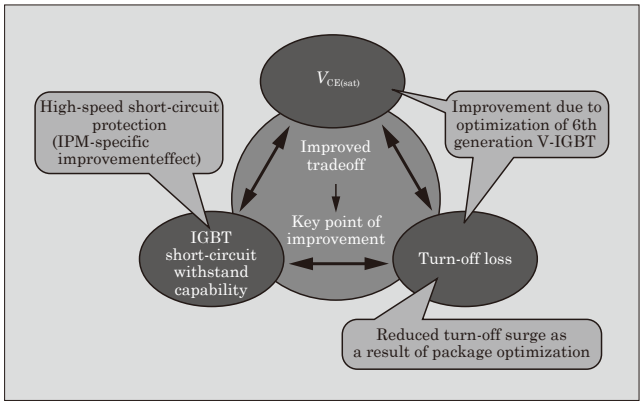

Also, optimization to improve the $V_{CE(sat)}$ tradeoff is being implemented with the goal of maintaining the same level of surge voltage as before, but with lower loss.

4.3 Lower turn-on loss

As a result of lower IGBT input capacitance, a new drive method for the control IC and improved temperature characteristics, as shown in Fig. 4, the tail of the collector-emitter voltage VCE becomes shorter and E_{on} is reduced by approximately 35%.

4.4 Comparison of radiation noise

A tradeoff relation exists between radiation noise and Eon, whereby loss can be reduced when di/dt is increased and radiation noise can be reduced when di/dt is decreased. Figure 5 shows an example of relative comparison test results as measured by Fuji Electric. Using a dummy load testing device, measurement was made during acceleration and deceleration operations. By employing the method for reducing turn-on loss described in section 4.3 and by optimizing the internal circuit wiring pattern in the package to reduce the radiating area, the peak value of radiation noise was approximately 3db lower than that of a conventional product. With this V-IPM, both lower E_{on} and lower radiation noise were realized.

4.5 Shorter dead time interval

In an inverter circuit, a dead time interval is

Fig.4 Turn-on waveform

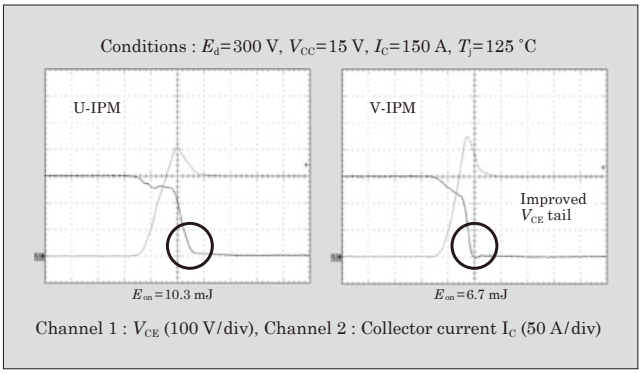

Fig.5 Comparison of radiation noise (results of relative comparison test at Fuji Electric)

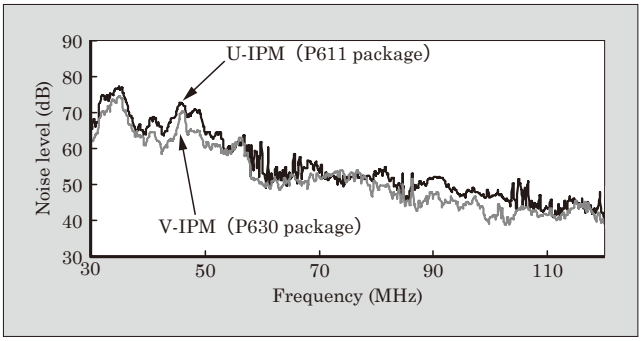

provided in order to prevent overlapping of the on-intervals of the upper and lower arms of the IPM. Shortening of the dead time interval is important for reducing waveform distortion and rotational unevenness. With the V-IPM, the switching time interval has been optimized by improving the temperature characteristics and reducing fluctuation during switching by the control IC. As a result of these techniques, the V-IPM realizes a minimum dead time interval of 1 μs at its IPM input section.

5. Protection Functions

5.1 Short-circuit protection

As described in section 4.2, the tradeoff relation between $V_{CE(sat)}$ and E_{off} in the IPM can be improved by diverting the short-circuit withstand capability of the IGBT chip to loss reduction. To realize this improvement, the speed at which the short-circuit protection operates must be increased. To speed up the protection circuit, the design of the V-IPM must ensure that the short-circuit protection function operates correctly with a shorter filter time. For this purpose, the sense voltage for the collector current monitor, which performs recognition sensing for the protection circuit, must be optimized.

With the IGBT, the sense ratio is adjusted to reduce the sense current and to stabilize the sense voltage during switching. Also, with the control IC, by changing to a new drive method from a gate resistance method based on the highly temperature dependent on-resistance of a MOSFET (Metal-Oxide-Semiconductor Field-Effect Transistor), the sense voltage is limited especially at high temperature conditions. As a result of these improvements, we successfully improved the tradeoff relation between loss and

Table 4 Alarm pulse width for each alarm cause

Alarm cause	Alarm pulse width
Over current protection (including short-circuit protection)	2 ms (standard value)
Low voltage protection	4 ms (standard value)
IGBT Chip over temperature protection	8 ms (standard value)

Fig.6 External appearance of package

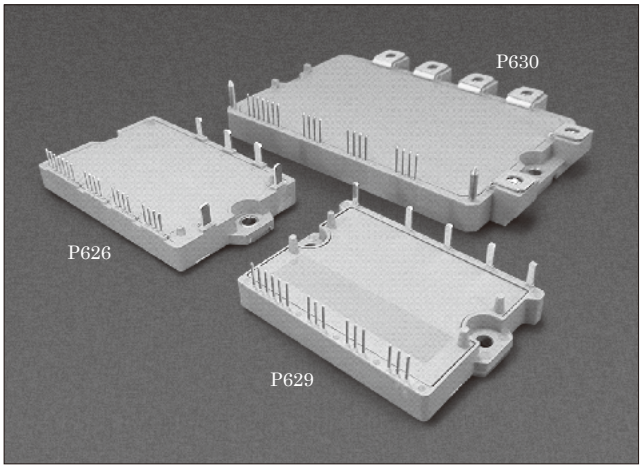

Fig.7 V-IPM block diagram

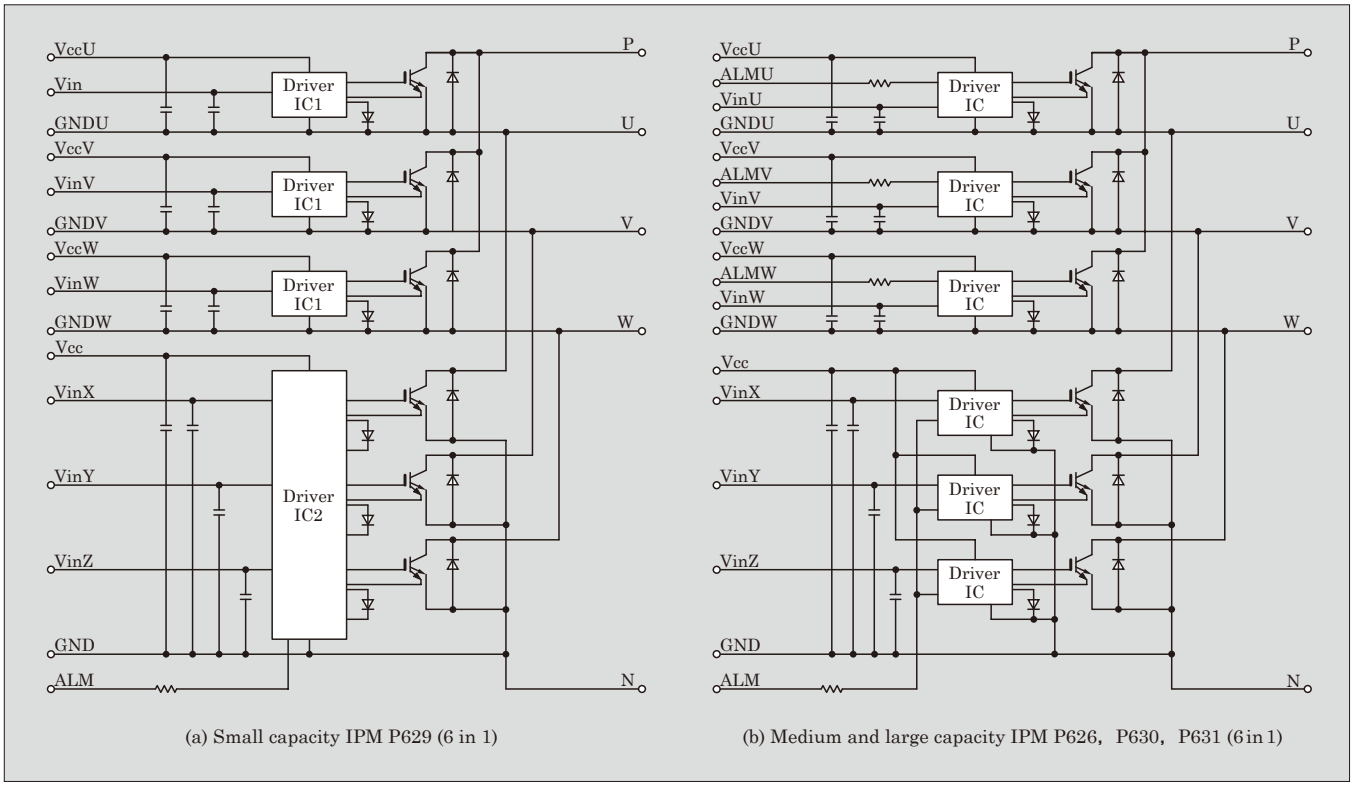

(a) Small capacity IPM P629 (6 in 1)

(b) Medium and large capacity IPM P626, P630, P631 (6 in 1)

short-circuit withstand capability.

5.2 Separate output for each alarm cause

A conventional IPM only has a single alarm pulse width of 2 ms, from which the cause of an alarm cannot be identified, but with the V-IPM, the alarm pulse width changes for each alarm cause, enabling the cause analysis to be performed more quickly when troubleshooting.

The alarm pulse widths for each V-IPM alarm cause are listed in Table 4.

6. Package

Figure 6 shows the external appearance of several packages. P629 is a small capacity package, P626 is a medium capacity and small size package, P630 is a medium capacity, thin package, and P631 (not shown) is a large capacity package.

The newly developed IPM has an external package shape designed in response to requests for thinner modules. A conventional package uses overhead crossing type bar wiring, and the wiring distance was shortened. With the new package, the internal circuit wiring is fabricated only from aluminum wire and the copper pattern on the insulating substrate to realize a thin package. Additionally, the internal inductance was reduced due to the mutual inductance effect from parallel PN lines. The resultant effect is that radiation noise is decreased, and turn-off surge does not become excessively large.

An additional advantage is that since a 50 A/600 V capacity is realized with the thin package of the P629, the height on the device is uniform, and the P629 can be used together with the P626. Moreover, the package design ensures sufficient insulation distance to ground and inter-phase insulating distance, and therefore, the insulating distance can be ensured without any special insulation design on the device side. All packages have RoHS compliant structures.

7. Block Diagram of IPM

Figure 7 shows block diagrams of IPMs. With a conventional small capacity type, current is detected with a shunt resistance that has been inserted into the N line, and therefore short-circuit protection could be implemented in the lower arm only. With the V-IPM, since all IGBTs use the sense current for detection, short-circuit protection of the upper arm device can be implemented. The P626, P630 and P631 packages are also provided with an alarm terminal on the upper arm, and alarm signals can be transmitted to the device side. Because P629 is designed to be compatible with the installation of previous models, an alarm signal terminal is not provided for the upper arm.

8. Postscript

Fuji Electric's FS-type "V-Series" IGBT chips (V-IGBT) having a trench gate structure and the "V-Series IPM" (V-IPM) that incorporates a new control IC into a new package have been introduced. The V-IPM realizes a compact size and high efficiency, and is able to meet market expectations. In the future, Fuji Electric intends to continue to concentrate on product development to satisfy market needs.

References

(1) Onozawa, Y. et al. Development of the next generation 1,200 V trench-gate FS-IGBT featuring lower EMI noise and lower switching loss. Proc. of ISPSD '07. p.13-16.

(2) Onozawa, Y. et al. Development of the 1,200 V FZ-diode with Soft Recovery Characteristics by the New Local Lifetime Control Technique. Proc. of ISPSD '08. p.80.

Superjunction MOSFET

Yasuhiko Oonishi † **Akihiko Ooi** ‡ **Takayuki Shimatou** ‡

ABSTRACT

600 V-class superjunction (SJ) MOSFETs (package : TO-220) with a maximum on-resistance of 0.16 Ω have been fabricated by using multi-epitaxial growth technology which has an excellent capability for controlling the doping concentration. By optimizing the doping concentration in the SJ structure, the fabricated SJ-MOSFET achieves an approximate 70% reduction in specific on-resistance compared to that of a conventional MOSFET "SuperFAP-E^3." This is the industry's highest level of specific on-resistance, and its value exceeds the theoretical limit for conventional MOSFETs. The avalanche withstand capability of the fabricated SJ-MOSFET has been also improved over the rated current by optimizing the doping profile of the SJ structure in the depth direction and the thickness and resistivity of the n-buffer layer.

1. Introduction

In recent years, as concern for protecting the global environmental has heightened, in the IT (information technology) sector, green IT has been attracting attention as a way to achieve power savings. In order to reduce the power loss of IT equipment, the power converters used with the IT equipment must be made more efficient. Consequently there is strong demand for low-loss power MOSFETs (Metal-Oxide-Semiconductor Field-Effect Transistors). The power MOSFETs used in power converters operate as switching devices and their associated dissipation loss consists of conduction loss while the power MOSFET is ON, and switching loss when the power MOSFET turns on and turns off. Generally, the conduction loss is dominant in applications having a low switching frequency, and the switching loss is dominant in applications having a high switching frequency. The on-resistance normalized to a unit area ($R_{on}\cdot A$) is used as a figure of merit for the conduction loss, and the gate-to-drain charge normalized to the on-resistance ($R_{on}\cdot Q_{GD}$) is used as a figure of merit for the switching loss. Thus, in order to reduce the dissipation loss of a power MOSFET, minimization of these figures of merit is strongly requested.

However, the breakdown voltage and $R_{on}\cdot A$ are associated with a theoretical limit that is determined by the material (in the case of silicon, this theoretical limit is known as the silicon limit), and it is not thought to be possible to obtain a $R_{on}\cdot A$ value that exceeds this theoretical limit. The super junction (SJ) structure is an innovative breakthrough that overcomes this limitation, and is attracting attention due to its ability to realize dramatically lower $R_{on}\cdot A$[1][2].

This paper describes the fabrication method and characteristics of Fuji Electric's newly developed 600 V-class SJ-MOSFET that realizes the lowest on-resistance in the industry and a high level of inductive load avalanche withstand capability.

2. Technical Trends of Power MOSFETs

Figure 1 shows the trends of $R_{on}\cdot A$ and $R_{on}\cdot Q_{GD}$ for 600 V-class power MOSFETs. As described above, a theoretical limit exists for the $R_{on}\cdot A$ of the power MOSFET, and therefore development efforts until now have focused on how to make the $R_{on}\cdot A$ approach the silicon limit as closely as possible. In order to reduce the $R_{on}\cdot A$, the drift resistance, which forms the silicon limit, was reduced and other resistance components were also reduced. The latter entails reducing the channel resistance and JFET (Junction Field-Effect Transistor) resistance by improving the cell density

Fig.1 Power MOSFET $R_{on}\cdot A$ and $R_{on}\cdot Q_{GD}$ trends

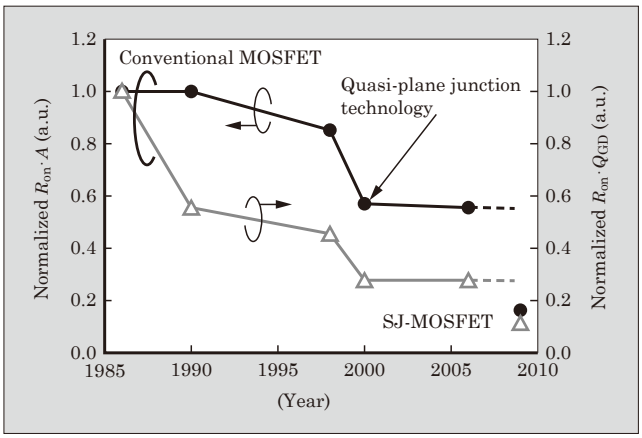

† Advanced Technology Laboratory, Fuji Electric Holdings Co., Ltd.

‡ Semiconductors Group, Fuji Electric Systems Co., Ltd.

of the surface MOSFET area and optimizing the cell structure, and the former entails reducing the drift resistance by optimizing the resistivity and thickness of the drift layer that ensure the inductive load avalanche withstand capability and the breakdown voltage. With a structure that uses a p-well region to ensure the inductive load avalanche withstand capability, there is a limit to extent with which the drift resistance can be reduced, but the application of quasi-plane junction technology enables this limit to be lowered[3]. With quasi-plane junction technology, instead of using a p-well structure, the drift resistance is reduced by narrowing the distance between p-base regions without increasing the JFET resistance, and by optimizing the p-base shape, an inductive load avalanche withstand capability equivalent to that of a p-well structure is guaranteed. By applying quasi-plane junction technology, the $R_{on} \cdot A$ of a conventional MOSFET has been improved to 110% of the silicon limit, and the $R_{on} \cdot Q_{GD}$ has also been improved significantly with the reduction in $R_{on} \cdot A$ and the narrower distance between p-base regions. Fuji Electric has applied this quasi-plane junction technology to commercialize the "SuperFAP-G Series" which is an easy-to-use successor of the "SuperFAP-E^3 Series[4]."

Recently, the SJ-MOSFET, which breaks through the silicon limit, has been attracting attention. As shown in Fig. 2, the SJ-MOSFET replaces the p-type and n-type regions in the drift layer of a conventional MOSFET with alternating regions of p-pillars and n-pillars, and because the impurity concentration of the n-type regions can be increased, the $R_{on} \cdot A$ can be reduced dramatically. Moreover, since the $R_{on} \cdot A$ can be reduced, the active area can be made smaller for the same on-resistance, thereby enabling the $R_{on} \cdot Q_{GD}$ to be reduced as well.

Fig.2 Structure of conventional MOSFET and SJ-MOSFET

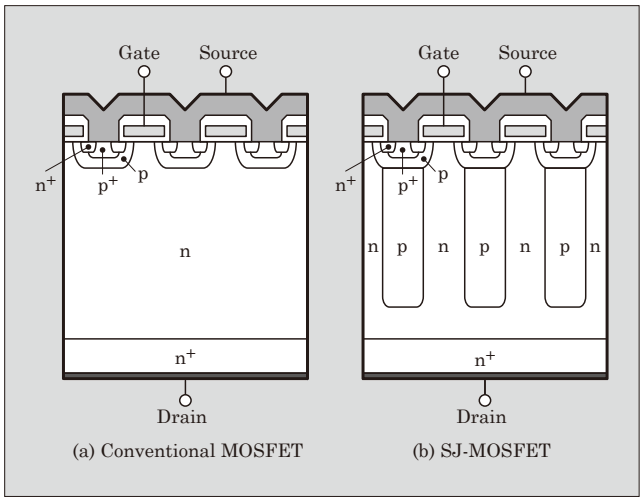

3. SJ-MOSFET Development

3.1 Multi-epitaxial growth technology

The SJ structure enables a dramatically lower value of $R_{on} \cdot A$, but because it is a charge compensation structure, it has the disadvantage of being unable to maintain its breakdown voltage unless a charge balance can be maintained between n-type and p-type regions. If the charge balance collapses, the breakdown voltage drops significantly and the rated voltage will not be maintainable. When fabricating an SJ-MOSFET, the impurity concentrations of the n-type and p-type regions must be controlled precisely. To reduce deviation of the breakdown voltage, the impurity concentration in the depth direction of the p-type region must be distributed. Therefore, the SJ structure is fabricated with a method of multi-epitaxial growth in which the processes of introducing impurities into a certain area by ion implantation, which has excellent impurity concentration control performance, and epitaxial growth are performed repeatedly[5]. Figure 3 shows the process flow of SJ structure fabrication by the multi-epitaxial growth method. First, an n-type layer having a low impurity concentration is grown epitaxially on an n-type substrate with consideration given to the thickness of the buffer layer (step 1). Next after completion of the fabrication of that layer, phosphorous (P) and boron (B) ions are injected into regions

Fig.3 SJ structure fabrication process flow using multi-epitaxial growth method

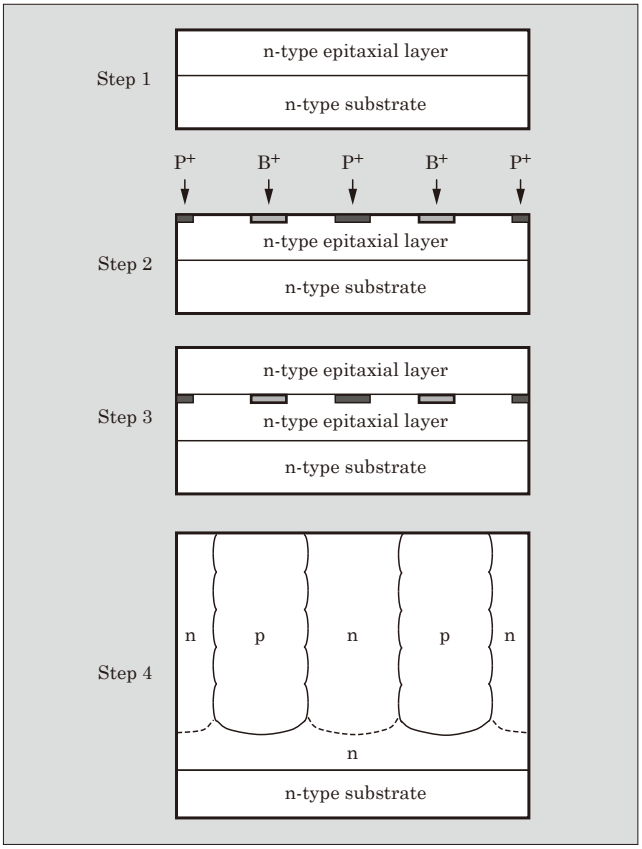

that will become n-type and p-type regions (step 2), and then an n-type layer having a low impurity concentration is grown epitaxially (step 3). Because the impurity concentrations in the fabricated n-type and p-type regions are determined by the dimensions of the resist for ion injection and by the accuracy of the ion injection itself, the impurity concentrations are easy to control. Steps 2 and 3 are repeated until a certain drift layer thickness is achieved, and then lastly, thermal diffusion is used to fabricate consecutive n-type and p-type regions. Thereafter, an ordinary DMOSFET (Double Diffused MOSFET) process is used to fabricate a DMOSFET on the surface of the SJ structure and create the SJ-MOSFET. Figure 4 shows an SCM (scanning capacitance microscopy) image of a cross-section of an SJ-MOSFET fabricated by the multi-epitaxial growth method. From the figure, it can be verified that an SJ structure, connected to both the p-type and n-type regions in the depth direction, has been fabricated.

Fig.4 SCM image of SJ-MOSFET cross-section

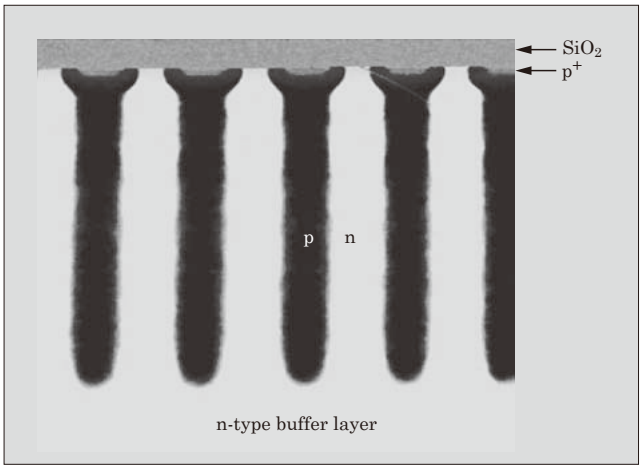

Fig.5 Comparison of figures of merit for conventional MOSFET and SJ-MOSFET

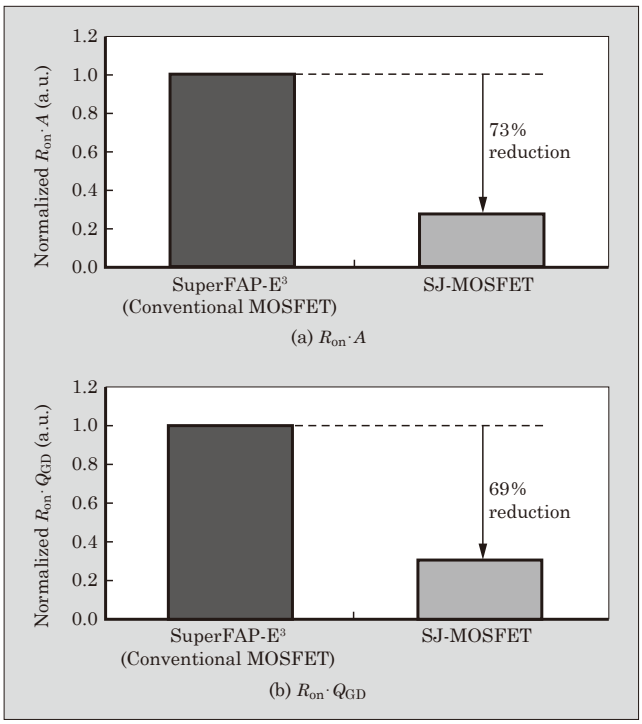

3.2 Improvement of R_{on}·A

Using the multi-epitaxial growth method, an SJ-MOSFET rated at 600 V and 0.16 Ω was developed. As shown in Fig. 5(a), the R_{on}·A of the developed SJ-MOSFET is approximately 73% lower than that of the SuperFAP-E^3, which is a conventional MOSFET. This is the industry's lowest level of R_{on}·A. A comparison of R_{on}·Q_{GD} is shown in Fig. 5(b). The R_{on}·Q_{GD} of the SJ-MOSFET is also approximately 69% lower than that of the SuperFAP-E^3. Moreover, the surface MOSFET structure of the SJ-MOSFET is based on the same concept as the SuperFAP-E^3 and inherits its ease-of-use. Figure 6 shows the output characteristics of the SJ-MOSFET for $V_{GS(th)}$=3.0 V.

Fig.6 Output characteristics of SJ-MOSFET

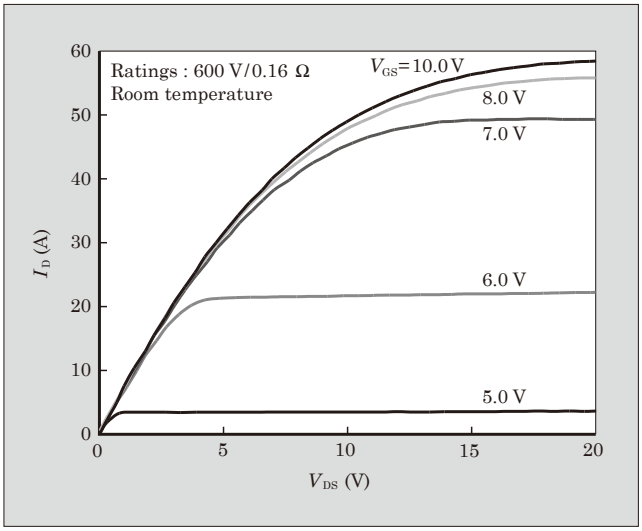

Fig.7 Inductive load avalanche waveform of SJ-MOSFET

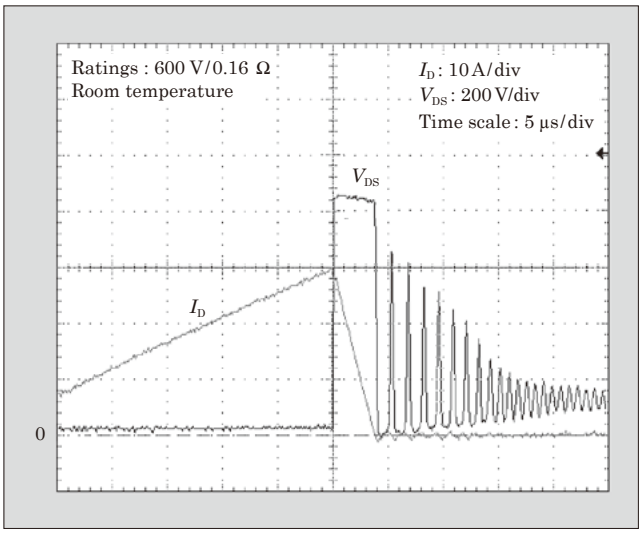

Fig.8 Power supply circuit for application evaluation

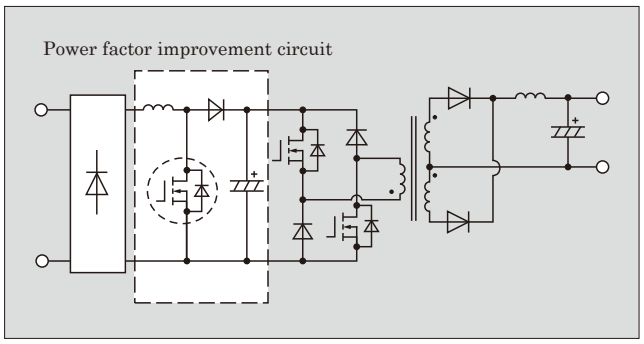

Fig.9 Comparison of power MOSFET dissipation loss (AC100 V input/400 W output)

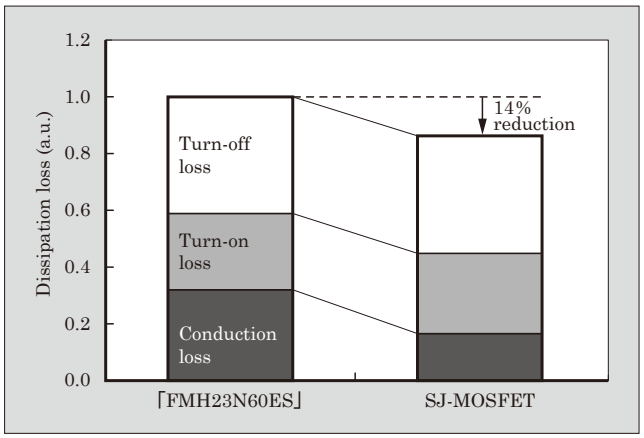

3.3 Improved inductive load avalanche withstand capability

It has been noted that the inductive load avalanche withstand current of an SJ-MOSFET is less than that of a conventional MOSFET. As a result of an optimized impurity concentration profile and n-type buffer layer in the depth direction of the SJ structure, the newly developed SJ-MOSFET guarantees an inductive load avalanche withstand capability of 150 A/cm^2 even under a balanced charge condition. Figure 7 shows a typical inductive load avalanche waveform of an SJ-MOSFET.

4. Application Results

An SJ-MOSFET (rated at 600 V/0.16 Ω) fabricated with the multi-epitaxial growth method and assembled in a TO-220 package was installed in the power factor improvement circuit (Fig. 8) of a 400 W-class ATX power supply (server power supply that conforms to the ATX standard), and the loss and temperature rise were evaluated. Figure 9 compares the power MOSFET area loss for an SJ-MOSFET and for the FMH23N60ES (rated at 600 V and 0.16 Ω), which has the lowest on-resistance among SuperFAP-E^3 series products and is housed in a TO-3P package. Compared to the conventional FMH23N60ES MOSFET, the SJ-MOSFET realizes 16% lower conduction loss and an approximately 14% reduction in total power loss. Moreover, the temperature rise has been confirmed to be approximately 5 °C lower, and an approximate 0.5% improvement in the total power conversion efficiency has also been verified. Although differences exist between the TO-220 and TO-3P packages, simple replacement with an SJ-MOSFET can expect to yield a lower dissipation loss and improved efficiency.

5. Postscript

An SJ-MOSFET (in a TO-220 package) that is fabricated by multi-epitaxial growth technology and rated at 600 V and 0.16 Ω has been developed. The SJ-MOSFET features an optimized impurity concentration in the SJ structure and an optimized n-type buffer layer to achieve the industry's lowest level of low $R_{on}\cdot A$, and a high inductive load avalanche withstand capability. In the future, Fuji Electric intends to develop a product lineup of low-loss SJ-MOSFETs and to contribute to efforts for protecting the global environment.

References

(1) Fujihira, T. Theory of Semiconductor Superjunction Devices. Jpn. J. Appl. Phys. Oct. 1997, vol.36, p.6254-6262.
(2) Deboy, G. et al. A New Generation of High Voltage MOSFETs Breaks the Limit Line of Silicon. Proc. IEDM. 1998, p.683-685.
(3) Kobayashi, T., et al, High-Voltage Power MOSFETs Reached Almost to the Si limit. Proc. ISPSD 2001, p. 99-102.
(4) Niimura, Y., et al. A Low Loss, Low Noise and Robust 500 to 900 V Class Power MOSFET with Multiple RESURF Guardring Edge Structure. Proc. PCIM. China, June 2009, p.150-155.
(5) Onishi, Y. et al. 24 mΩ•cm^2 680 V Silicon Superjunction. MOSFET. Proc. ISPSD. June 2002, p.241-244.

High Reliability Power MOSFETs for Space Applications

Masanori Inoue † **Takashi Kobayashi** † **Atsushi Maruyama** †

ABSTRACT

We have developed highly reliable and radiation-hardened power MOSFETs for use in outer space applications in satellites and space stations. The largest difference between these newly developed Rad-Hard Power MOSFETs and general-use MOSFETs is that they have excellent durability against high energy charged particles and ionizing radiation. To provide increased durability, electrical characteristics had been sacrificed in the past. With this device, however, to provide durability against high energy charged particles, a drift diffusion model was modified so as to enable simulation of the mechanism. A power MOSFET designed for use in outer space applications and having the world's top level performance is realized by providing a thick epitaxial layer with low specific resistance as a countermeasure to ensure durability against SEB (single event burn-out).

1. Introduction

It is well known that the benefits derived from outer space applications such as communication satellites, weather satellites, GPS (Global Positioning System) and earth observation are pervasive in society today.

The electronic devices and switching power supplies installed in artificial satellites are required to be both highly efficient so that the limited electric power in outer space can be utilized effectively and to have a reduced part count so as to ensure reliability as a system. Accordingly, power MOSFETs (Metal-Oxide-Semiconductor Field-Effect Transistors) are required to have low loss and, in a space environment, high reliability with tolerance[2] to ionizing radiation[1], high-energy charged particles and the like. Particularly, in outer space, most semiconductor components exhibit a significant degradation in their electrical characteristics, and products that are commonly used in terrestrial applications are unable to provide guaranteed reliability in space.

At the time when Fuji Electric began to develop power MOSFETs for space applications, there already existed much research[1],[2] into the degradation of power MOSFET characteristics caused by ionization radiation and countermeasures to prevent that degradation. However, the mechanism of the SEB (single event burnout) phenomenon, in which high-energy charged particles cause instantaneous burnout, was unknown. Consequently, Fuji Electric's 1st generation of space-use power MOSFETs sacrificed electrical characteristics for SEB tolerance, but by employing an estimated SEB mechanism as described below, Fuji Electric has recently developed a 2nd generation of high-reliability space-use power MOSFETs having electric characteristics that are equivalent to those of consumer-use power MOSFETs. Figure 1 shows the external appearance of these power MOSFET products, and Table 1 lists their main characteristics.

The results of this achievement are described herein.

2. Fuji Electric's Contribution to Space Development

Fuji Electric's contribution to space development began in the 1980s with involvement in the development of the "H-Ⅱ" rocket which was developed and built exclusively in Japan by combining the technical expertise of various Japanese manufacturers under the guidance of the former NASDA (National Space Development Agency of Japan). Fuji Electric developed and supplied high-reliability BJTs (bipolar junction transistors) for this effort, and contributed to the successful launch of the first H-Ⅱ rocket in 1994.

Fuji Electric's 1st generation space-use power MOSFETs are also installed in the International Space

Fig.1 External appearance of power MOSFET products

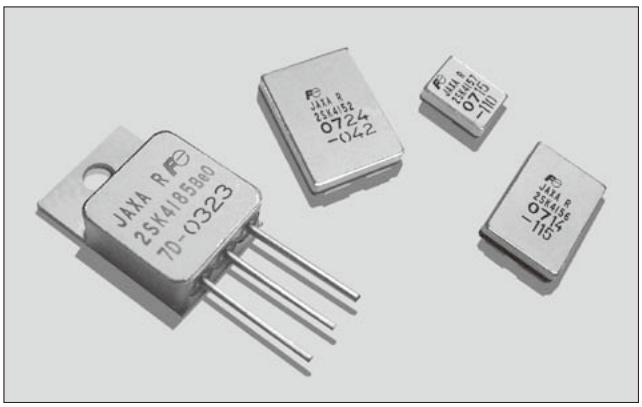

† Semiconductors Group, Fuji Electric Systems Co., Ltd.

Table 1 Product list

Model	V_{DSS} (V)	I_D (A)	$R_{DS(on)}$*1 max. (Ω)	P_D*2 (W)	V_{GS} (V)	$V_{GS(th)}$ (V)	Q_g max. (nC)	Radiation level (krad)	Package type
JAXA R 2SK4217	100	42	0.013	250	±20	2.5 - 4.5	220	100	SMD-2
JAXA R 2SK4218	100	42	0.028	150	±20	2.5 - 4.5	100	100	SMD-1
JAXA R 2SK4219	100	15	0.064	70	±20	2.5 - 4.5	50	100	SMD-0.5
JAXA R 2SK4152	130	42	0.017	250	±20	2.5 - 4.5	220	100	SMD-2
JAXA R 2SK4153	130	39	0.039	150	±20	2.5 - 4.5	100	100	SMD-1
JAXA R 2SK4154	130	15	0.089	70	±20	2.5 - 4.5	50	100	SMD-0.5
JAXA R 2SK4155	200	42	0.026	250	±20	2.5 - 4.5	220	100	SMD-2
JAXA R 2SK4156	200	32	0.062	150	±20	2.5 - 4.5	100	100	SMD-1
JAXA R 2SK4157	200	14	0.148	70	±20	2.5 - 4.5	50	100	SMD-0.5
JAXA R 2SK4158	250	42	0.038	250	±20	2.5 - 4.5	220	100	SMD-2
JAXA R 2SK4159	250	26	0.091	150	±20	2.5 - 4.5	100	100	SMD-1
JAXA R 2SK4160	250	12	0.223	70	±20	2.5 - 4.5	50	100	SMD-0.5
JAXA R 2SK4188	500	23	0.18	250	±20	2.5 - 4.5	300	100	SMD-2
JAXA R 2SK4189	500	10	0.48	150	±20	2.5 - 4.5	120	100	SMD-1
JAXA R 2SK4190	500	4.5	1.15	70	±20	2.5 - 4.5	48	100	SMD-0.5

*1 $R_{DS(on)}$: V_{GS}=12 V, *2 P_D : T_C=25 ˚C

Table 2 Requirements for space-use power MOSFETs

Requirement		Actual or targeted performance		
		Actual performance of consumer-use MOSFETs	Space-use MOSFETs	
			Actual performance of 1st gen. MOSFETs	Targeted performance of 2nd gen. MOSFETs
Electrical characteristic	Break down voltage (V)	250 V	500 V	250 V
	On-resistance	○	△	○
Long-term reliability		△	○	○
Tolerance to radiation (TID)		×	○	○
Tolerance to high-energy charged particles (SEB tolerance)		×	○	○

○ : Satisfied requirements △ : Slightly below requirements
× : Did not meet requirements

Station that is being assembled in orbit through cooperation from the United States, Russia, Japan, Canada and Europe. Approximately 3,000 of these MOSFETs are installed in the Japanese Experimental Module known as "Kibo," and these MOSFETs have continued to operate properly ever since their insertion into orbit in March 2008.

3. Development of 2nd Generation Space-use Power MOSFETs

The aforementioned 1st generation space-use power MOSFETs have sufficient tolerance to ionization radiation. However, in order to ensure adequate SEB tolerance, the element breakdown voltage was increased. But, increasing the element breakdown voltage leads to increased on-resistance and greater loss.

An objective of the 2nd generation of space-use power MOSFETs was to enhance the SEB tolerance and to realize electrical characteristics that are equivalent to those of consumer-use power MOSFETs. Table 2 lists the requirements for space-use power MOSFETs.

Fig.2 Internal structure of power MOSFETs for space applications

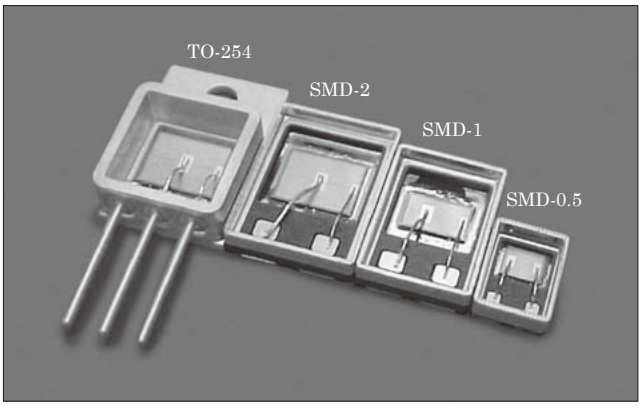

3.1 Technical challenges of power MOSFETs for space applications

Consumer-use power MOSFETs have excellent electrical characteristics but are not compatible with ionizing radiation and high-energy charged particles. Because the 1st generation of space-use power MOSFETs had insufficient SEB tolerance, the breakdown voltage had to be raised to 500 V, and the on-resistance was sacrificed.

The reduction of on-resistance while ensuring SEB tolerance and TID (total ionizing dose) tolerance, as well as ensuring long-term reliability, were challenges for the 2nd generation of space-use power MOSFETs.

With the measures described in paragraphs (1) and (2) below, requirements of the 1st generation space-use

power MOSFET can be satisfied. The SEB measure described in paragraph (3) is a special feature of the 2nd generation space-use power MOSFETs.

(1) Use of hermetically sealed package to realize long-term reliability

Reliability is improved with the use of a metal hermetically sealed package. A sintered compact of copper-tungsten (Cu-W), having a coefficient of thermal expansion that is extremely close to that of silicon (the raw material of the MOSFET chip), is used in the package frame (area in which the MOSFET chip is installed) to improve the temperature cycling tolerance. Moreover, as shown in Fig. 2, the interior of the hermetically sealed package is hollow, and this void is filled with dry nitrogen gas to protect the power MOSFET chip from extrinsic degradation.

(2) Use of low-temperature process to ensure TID

Generally, when a power MOSFET for terrestrial applications is used in an environment of ionizing radiation, the breakdown voltage decreases and a shift occurs in the threshold voltage V_{th} of the gate that controls the on-off switching of the power MOSFET. The degradation of the power MOSFET's characteristics due to TID is a phenomenon caused by electric charge trapped in the oxide film.

In the manufacture of power MOSFETs for space applications, the heat treatment after fabrication of the oxide film is performed at a low temperature in order to decrease the amount of electric charges trapped in the oxide film and to provide a TID tolerance of 1,000 Gy which is equivalent to the ionizing radiation exposure for 10 years in a geostationary orbit.

(3) Use of 2-step epitaxial layer structure to ensure SEB

Since about 1986, the phenomena of semiconductor device malfunction and sudden damage due to high-energy charged particles (such as nickel (Ni) ions, for example) have been reported. Such phenomena can be caused by a single high-energy charged particle, and are collectively known as single event effects (SEEs). One type of a SEE that affects power MOSFETs is SEB, which has been reported as the instantaneous burnout of a device.

At the time when Fuji Electric began development of 2nd generation space-use power MOSFETs in 1992, the mechanism behind the SEB phenomenon was not understood. Fuji Electric began to analyze the mechanism using simulation technology.

Fig.3 Distribution of electric field intensity and electron-hole pair generation

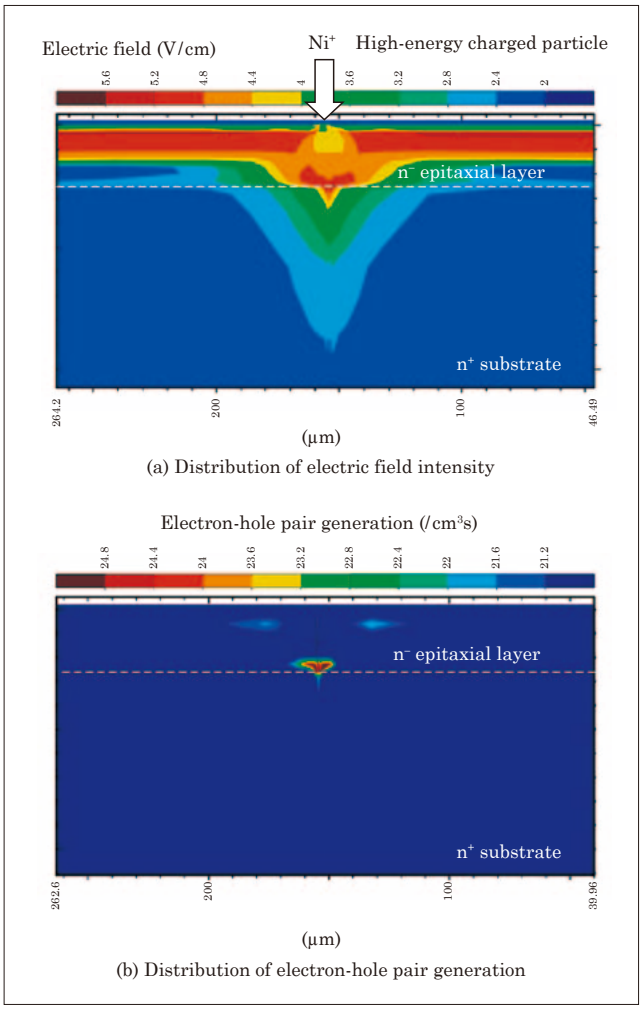

(a) Distribution of electric field intensity

(b) Distribution of electron-hole pair generation

3.2 Estimated SEB mechanism

The SEB phenomenon could not be reproduced with a conventional simulation model, but this issue was overcome by performing the simulation with a corrected drift-diffusion model. From our analysis of the simulation, the following can be understood.

Figure 3 shows the distribution of electric field intensity and the distribution of electron-hole pair gen-

Fig.4 Distribution of electric potential at incidence of high-energy charged particles

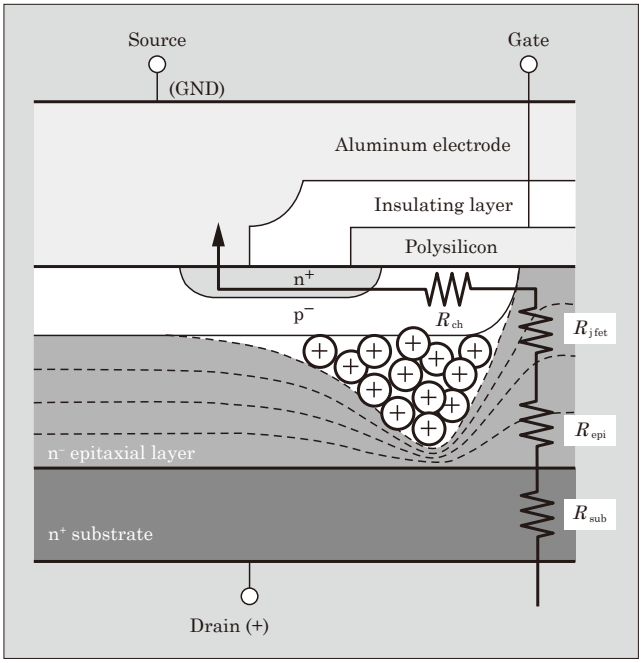

eration. Electron-hole pairs are generated along the trajectory of a high-energy charged particle. In the vicinity of a collision of a high-energy charged particle to the n^+ substrate, a high electric field region is formed and a large quantity of electron-hole pairs is generated. An excess of holes is formed up until the boundary between the epitaxial layer and the n^+ substrate, and at this tip, the electric field is strong, and electron-hole pairs are generated actively.

From these findings, the SEB mechanism can be estimated as follows.

(1) As a result of the incident high-energy charged particles, holes from the generated electron-hole pairs are supplied as base current to operate a parasitic npn transistor.

(2) The excess of holes increase along the trajectory of the incident high-energy charged particles (Fig. 4), and the base of the parasitic npn transistor is pushed-out. As for the effective edge of the base, a high electric field region is formed to block the path with the n^+ substrate.

In this region, a super high-density current flows and, as a result, even at voltages less than the breakdown voltage, dynamic avalanching occurs easily and electron-hole pairs are generated.

(3) The generated holes are supplied again as base current, which facilitates the operation of the parasitic npn transistor.

(4) Thus, the generation of holes due to dynamic avalanching in the high electric field region in the vicinity of the boundary between the substrate and epitaxial layer causes a positive feedback action similar to that of a thyristor, and leads to damage.

4. Proposed Structure to Prevent SEB

In consideration of the aforementioned mechanism, the following structure to prevent SEB was proposed and implemented.

Fig.5 Dependency of SEB tolerance on n^- epitaxial layer thickness

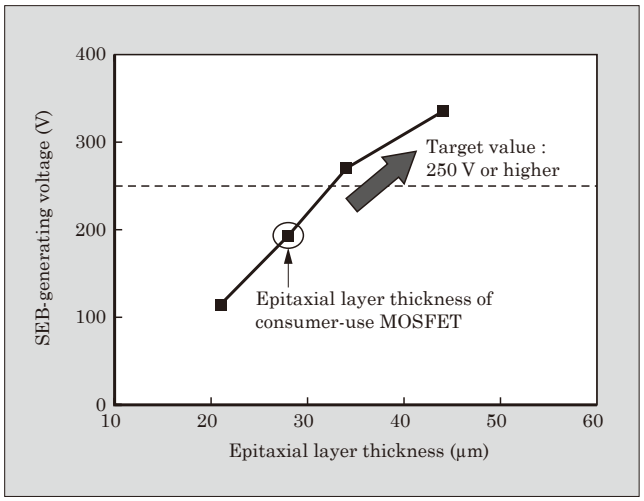

With this structure, it is thought that even if the base is pushed-out, as long as sufficient distance to the n^+ substrate is ensured, an electric field will not reach a high enough value to cause dynamic avalanching, and the generation of SEB can be reduced. To verify the effectiveness of the proposed structure, actual prototypes of MOSFETs with different epitaxial layer thicknesses were fabricated and tested. As the test results, Fig. 5 shows the dependency of epitaxial layer thickness on SEB-generating voltage.

To obtain a breakdown voltage of 250 V with this structure, an epitaxial layer thickness of approximately 29 μm is needed, but with this design, SEB occurred at about 200 V, which is approximately 60% of the breakdown voltage. On the other hand, with a device having a thicker epitaxial layer, we found that the SEB-generating voltage is higher and that the desired effect could be obtained. Based on these test results, the targeted SEB-generating voltage could be attained by setting the epitaxial layer thickness to 32 μm.

On the other hand, this measure sacrifices (increases) the on-resistance, which is a critical characteristic of power MOSFETs. Figure 4 also shows the on-resistance configuration of a power MOSFET. The n^- epitaxial layer is the current path when the power MOSFET turns on and operates, and is directly linked to an increase in on-resistance. The on-resistance R_{epi} of the n^- epitaxial layer accounts for a large percentage of the total on-resistance, and in the case of a 250 V

Fig.6 Cross-section of active area of 2nd generation space-use power MOSFET that uses a 2-step epitaxial layer structure

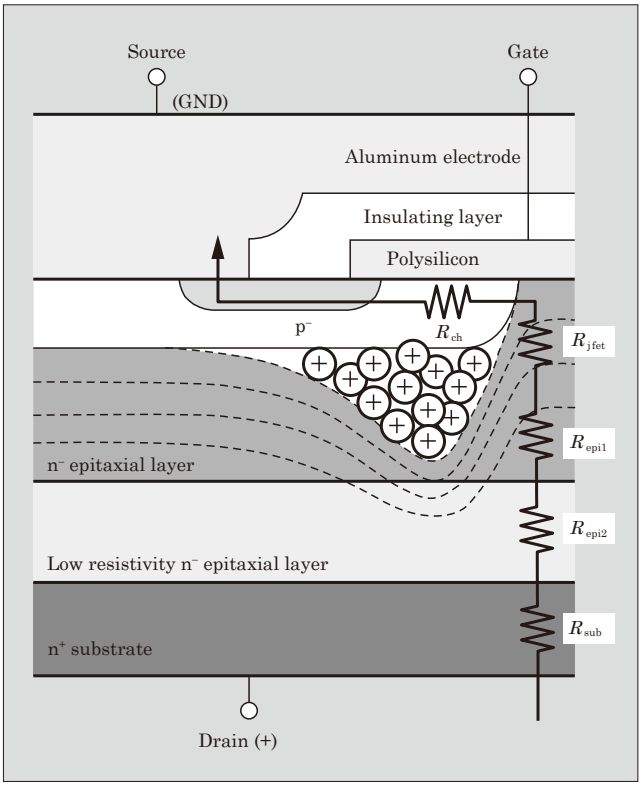

rated device, for example, accounts for approximately 80% of the total.

To avoid this increase in on-resistance, instead of simply increasing the thickness of the epitaxial layer, we proposed a 2-step epitaxial layer structure (Fig. 6) that is provided with an n⁻ epitaxial layer of low resistivity R_{epi2}.

With this structure, a resistivity higher than that of an n+ substrate can be obtained even with an epitaxial layer of low-resistivity, and an effect equivalent to increasing the epitaxial layer thickness is thought to be obtainable. Moreover, as a result of the large quantity of electrons injected from the parasitic npn transistor and the relative difference in impurity concentrations (corresponding to the resistivity) of the epitaxial layers, the base is pushed out and a high electric field is formed, and therefore, increasing the impurity concentrations of the epitaxial layers (lowering the resistivity) is also expected to have the effect of suppressing the generation of a high electric field.

Fig.7 Dependence of SEB capacity on electrical resistance of epitaxial layer

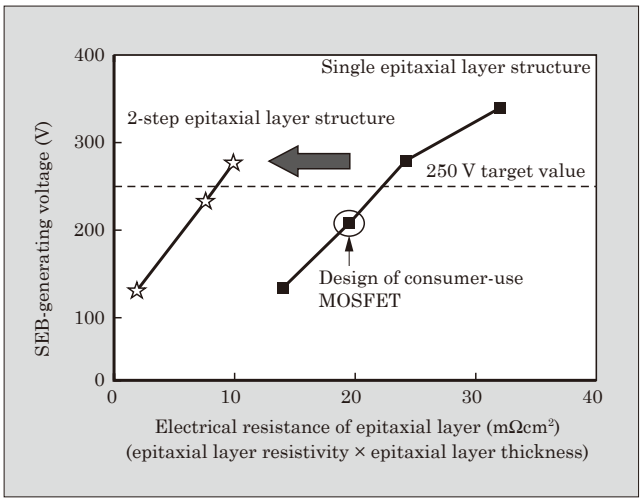

Fig.8 Breakdown voltage dependency of on-resistance

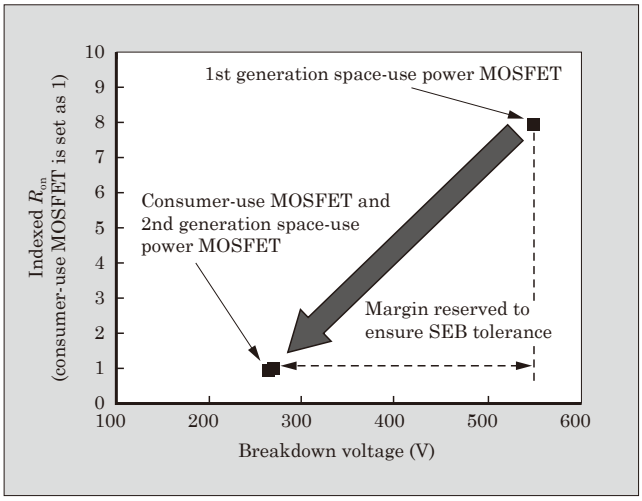

Figure 7 shows the relationship between the electrical resistance of the epitaxial layer and the voltage at which SEB is generated. With the innovative 2-step epitaxial layer structure, the targeted SEB-generating voltage can be achieved even if the resistance of the entire epitaxial layer is lowered by about 50%.

The application of this 2-step epitaxial layer structure enables the SEB tolerance to be ensured and the increase in on-resistance to be minimized (3% or less). Figure 8 shows the tradeoff between breakdown voltage and R_{on}. The breakdown voltage margin that had been reserved in order to ensure SEB tolerance is eliminated, and a 2nd generation high-reliability space-use power MOSFET having excellent on-resistance characteristics was developed.

5. Postscript

By successfully estimating the SEB mechanism, we have minimized the increase in on-resistance and commercialized a space-use high-reliability power MOSFET product having electrical characteristics equivalent to those of a consumer-use power MOSFET. This paper has described a 250 V-class product, but a lineup that includes 100 V, 130 V, 200 V and 500 V-class products using this technology is available.

The 2nd generation space-use high-reliability power MOSFET realizes the top level of performance in the world. In the future, Fuji Electric intends to continue to make contributions to space development.

References

(1) Gover, J. E. Basic Radiation Effects in Electronics Technology. Colorado Springs, CO, Proc. 1984 IEEE NSREC Tutorial Short Course on Radiation Effects. July 22, 1984.
(2) Waskiewicz, A. E. et al. Burnout of Power MOSFET with Heavy Ions of CaliFornium-252. IEEE Trans. Nucl. Sci. Dec. 1986, vol.NS-33, no.6, p.1710-1713.

Pressure Sensor for Exhaust Systems

Katsuyuki Uematsu † **Hiroko Tanaka** † **Hirofumi Kato** †

ABSTRACT

Exhaust gas regulations for motor vehicles are becoming stricter year-after-year, and as internal combustion engines are being made more efficient and their exhaust gas reduced, there is increased demand for pressure sensing in the exhaust systems of diesel engine vehicles. Applying a single-chip semiconductor pressure sensor fabricated by a CMOS process, which has been successfully used for manifold pressure measurement, Fuji Electric has developed an exhaust system pressure sensor capable of withstanding an exhaust gas environment containing corrosive substances. The newly developed sensor, in a DIN standard SO_2 gas test, exhibited the ability to withstand corrosion that is more than 2.5 times greater than that of conventional sensors, and is suitable for use in absolute pressure sensing and relative pressure sensing applications.

1. Introduction

Industrial development and expanded distribution in the BRIC countries (Brazil, Russia, India and China) and elsewhere are ongoing. The associated increase in economic activity on a global scale is acerbating the problems of global warming caused by the emission of greenhouse gases such as carbon dioxide (CO_2) and acid rain and air pollution caused by nitrogen oxides (NO_x) and sulfur oxides (SO_x).

As exemplified by the Green New Deal policies in the US, and Japan's announced intent to reduce CO_2 exhaust emissions by 25% by the year 2020, environmental issues are being addressed as national and global problems. With the establishment of strict targets for emission regulation, the development of new environmental technologies and the accompanying economic activity are expected to provide opportunities for environmental businesses.

In particular, environmental measures implemented by the automobile industry, which account for a major portion of the economic activities relating to industry and distribution, are being watched closely. In order to meet the exhaust emission regulations which are being strengthened from year to year, automobile manufacturers have concentrated their efforts on increasing the efficiency and realizing cleaner emissions of combustion engines, and on developing hybrid vehicles and electric vehicles.

2. Fuji Electric's Pressure Sensors

To achieve cleaner emissions and more efficient fuel consumption of automobiles, the engine control must be made more accurate. In present-day automobiles, engine information such as the load status, aspiration and temperature acquired from sensors installed at various locations in the engine is used to control combustion electronically to realize an optimal air-fuel ratio.

Automotive pressure sensors attached to the intake manifold of an engine and used primarily for measuring intake pressure have helped to make engine control more efficient. Also, in addition to intake pressure measurement sensors, multiple other pressure sensors, such as boost pressure sensors for turbo chargers and super chargers, clogging detection sensors for air filters and barometric pressure sensors[(1)] for compensating the intake pressure at higher altitudes at which the air becomes thinner, are being used.

Fuji Electric began mass-producing manifold absolute pressure (MAP) sensors for automobile engines in 1984. The first sensor had many parts, including a circuit for adjusting the characteristics of a piezo-resistive gauge and a circuit board on which SMDs (surface mounted devices) for dealing with EMC (electromagnetic compatibility) such as chip capacitors, chip resis-

Fig.1 Sensor unit of pressure sensor

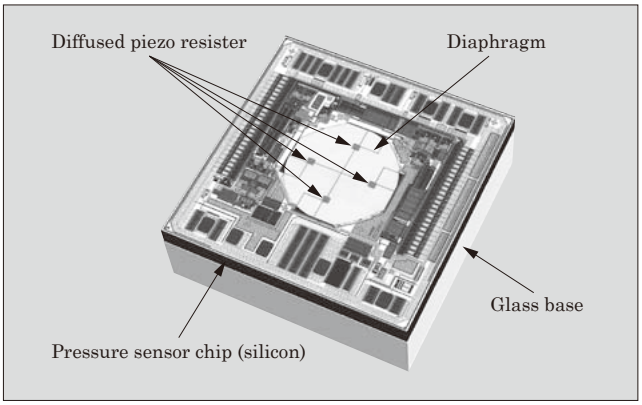

† Semiconductors Group, Fuji Electric Systems Co., Ltd.

tors and the like are mounted, and the parts had many electrical contacts[2].

To enhance the reliability by reducing the number of parts, Fuji Electric developed a pressure sensor in which the sensing unit, amplifier circuit, temperature characteristic compensation circuit and EMC protection devices are integrated into a single chip using a standard semiconductor CMOS (complementary metal-oxide-semiconductor) process. This single-chip type of pressure sensor has been deployed in the market mainly as a MAP sensor since 2002.

Figure 1 shows an overview of the sensor unit of this pressure sensor, and Fig. 2 shows the cross-sectional structure of this pressure sensor.

Diffused piezo-resistors are fabricated on a diaphragm at the same time as the IC process is performed, and a Wheatstone bridge is configured with four diffused piezo-resistors. The diaphragm ensures a high burst pressure and is formed, using Fuji Electric's proprietary silicon etching process, in a precise round shape.

When the application of pressure causes the diaphragm to flex, the resistance values of the diffused piezo-resistors come to change due to the piezo-resistive effect, and the output of the Wheatstone bridge changes. As a result of this principle, the pressure quantity can be converted into a voltage. Moreover, a high precision amplifier for amplifying the signal output from the Wheatstone bridge and an adjustment circuit for compensating the sensor characteristics are built on a single chip. Additionally, protection devices for protecting internal circuits from surges generated by the automobile engine control system, and from static electricity during the assembly process and electromagnetic noise from external sources, and so on, are all provided on a single chip[3].

As shown in Fig. 3, the sensor unit is embedded in a resin package, and electrical and mechanical connections are made to the exterior. The sensor cell package is made from PPS (polyphenylene sulfide), which is used for automotive parts and has excellent resistance to acid, and the sensor chip unit, lead frame and wires are coated with fluoro silicone gel, which has excellent chemical resistance and oil resistance.

Fig.2 Cross-sectional structure of pressure sensor unit

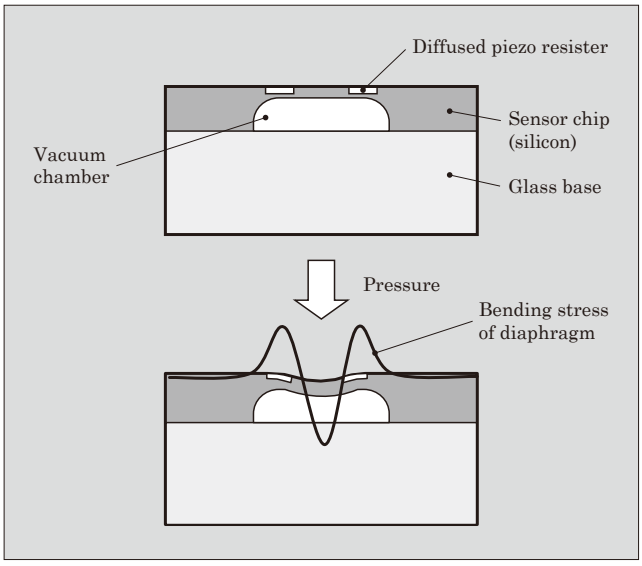

Fig.3 Structure of pressure sensor cell

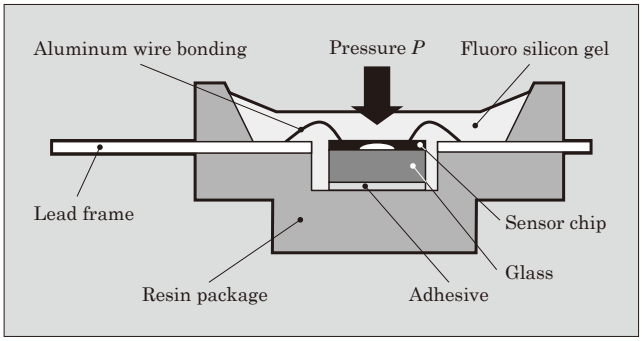

3. Application to Pressure Sensors for Exhaust System

Exhaust emissions regulations for automobiles have been strengthened year after year since the Muskie Act in the 1970s, and in Japan, Post-New Long-Term exhaust emission regulations came into effect in 2009. In Europe, the EURO5 emission regula-

Fig.4 Changes in NO_x and PM exhaust emission regulations for diesel passenger cars
(Prepared by Fuji Electric and based on documents from the Japanese Ministry of Land, Infrastructure and Transport, the Japanese Ministry of Economy, Trade and Industry, and Japan Automobile Manufacturers Association)

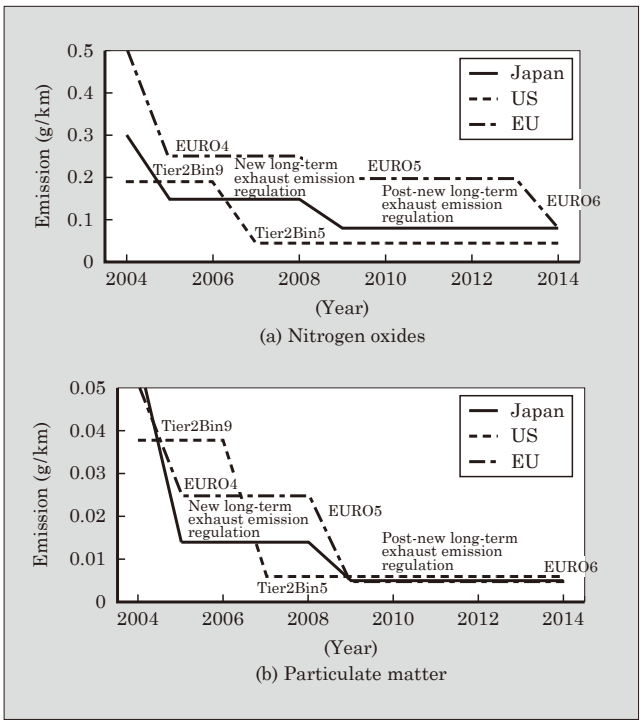

tions came into effect in 2009, and the EURO6 regulations are slated to come into effect in 2014. Figure 4 shows the changes in exhaust emission regulations for diesel passenger cars.

Aiming to improve fuel economy and to reduce CO_2 greenhouse gas emissions, diesel automobiles are in high demand chiefly in Europe and account for more than half of the total number of automobiles sold in Europe. Diesel automobiles have much better fuel economy and lower CO_2 emissions than gasoline-powered automobiles, but the NO_x emissions that accompany their higher combustion temperature and PM (particulate matter) emissions due to imperfect combustion are problems.

Recently, a DPF (diesel particulate filter) used to remove PM contained in exhaust gas has begun to be installed mainly in diesel automobiles. A pressure sensor is used to sense clogging of this filter. Additionally, an EGR (exhaust gas recirculation) system in which a portion of exhaust gas is recirculated to the intake side so as to control combustion has begun to be utilized, and pressure sensors have come to be used to measure the pressure of exhaust gas (Fig. 5).

The sensors used in these exhaust systems must be protected from corrosive matter such as acid caused by the NO_x and SO_x contained in the exhaust gas, and incompletely combusted fuels and oils.

Fuji Electric's newly developed pressure sensor for exhaust systems uses a conventional intake pressure sensor and implements the "corrosion free design" required for exhaust system pressure sensors (Fig. 6).

Fig.5 Engine intake/exhaust system and pressure sensor

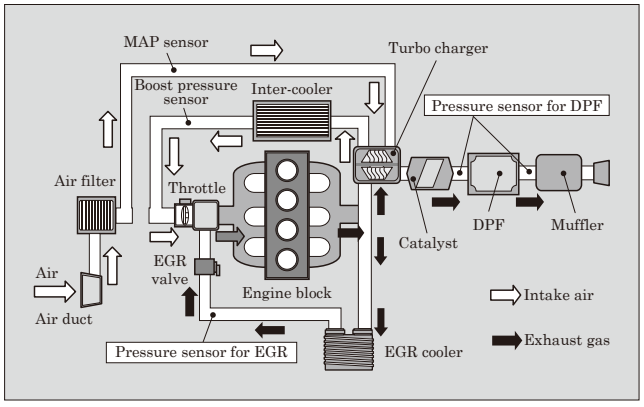

Fig.6 Exhaust system pressure sensor

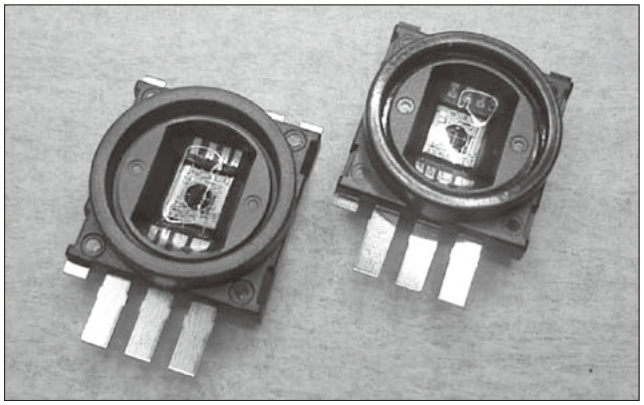

4. Corrosion Resistant Design to Protect Against Corrosive Matter in Exhaust Gas

The corrosion resistance required of exhaust system pressure sensors has been achieved by implementing the following.

(1) Gold plating of electrode pads on the chip
(2) Gold wire bonding between the chip and lead frame
(3) Gold plating of lead frame for the resin case

Details of these techniques and their evaluation results are described below.

4.1 Corrosion resistant design of sensor chip

The electrode pads of the semiconductor chip, which is fabricated by Fuji Electric's standard CMOS process, are made from an aluminum alloy. If SO_x gas and steam contained in the exhaust gas permeate into the fluoro silicone gel on the chip, sulfuric acid is generated by the mechanism listed below, and the aluminum corrodes.

$$2SO_2 + O_2 \rightarrow 2SO_3$$
$$SO_3 + H_2O \rightarrow 2H^+ + (SO_4)^{2-}$$
$$2Al + 6H^+ \rightarrow 2Al^{3+} + 3H_2$$

Therefore, the electrode pads of the chip are coated with a gold plating layer to form a corrosion resistant structure. Figure 7 shows the cross-sectional structure of the electrode pads and the gold plating on the chip. In order to prevent aluminum and gold from diffusing between the aluminum alloy layer and the gold plating layer, a barrier layer of a titanium-tungsten (Ti-W) alloy is provided (for the purpose of explanation, the proportion of horizontal and vertical length in the figure differs from that of an actual chip).

Moreover, conventionally, the chip and lead frame were bonded together by aluminum wire, but because the same chemical reaction would cause the wire to corrode and possibly break, gold wire was used for the

Fig.7 Corrosion resistant structure of sensor chip electrode pads

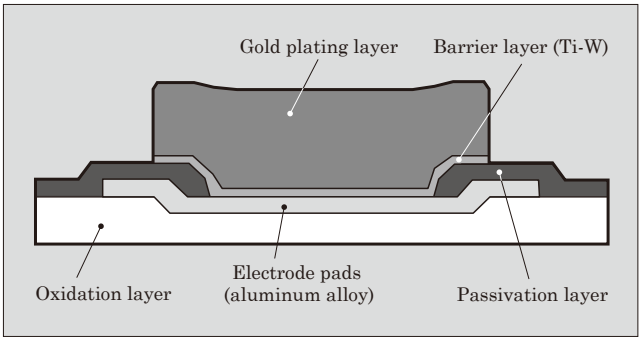

Fig.8 Structure of exhaust system pressure sensor

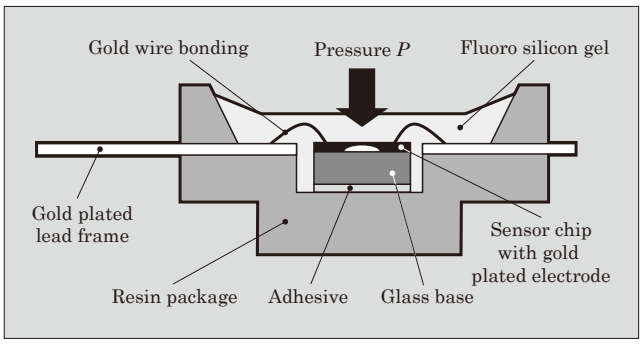

Fig.9 SO_2 gas test results

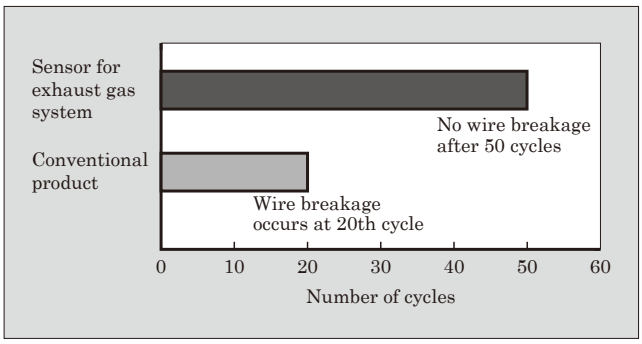

Table 1 SO_2 gas test conditions (DIN50018-SFW1.0S)

Theoretical SO_2 concentration at start of cycle (vol. %)			0.33*
Condensate climate			DIN50018-SFW 1.0S
Cycles	1st test process (h)		8 (including heating)
	2nd test process (h)		16 (including cooling) (test box is open or ventilated)
	Total (h)		24
Test room conditions	1st test process	Temperature (°C)	40 ± 3
		Relative humidity (%)	Approximately 100 (forming condensation on the test material)
	2nd test process	Temperature (°C)	18 to 28
		Relative humidity (%)	75 (max.)

* : The theoretical SO_2 concentration, in the case of a test box having a 300 L volume, corresponds to 1.0L of SO_2 added for each cycle.

new sensor.

4.2 Corrosion resistant design of the package

In an existing pressure sensor cell package, the lead frame is plated with nickel, but depending on the surface condition of the plating, the leads may become corroded by acid that has formed from the exhaust gas, resulting in a break in the electrical connections to the exterior. Therefore, a gold layer is plated on top of the nickel plating to create a structure that prevents corrosion.

Since acid formed from corrosive gas reaches the interface between the lead frame and resin, the side surfaces, i.e., the cut surfaces, of the lead frame that are implanted into the resin must be corrosion-resistant. After press-cutting of the lead frame, a gold plating process is performed, and the cut edge surfaces are gold-plated (Fig. 8).

4.3 Corrosion resistance test results

To evaluate the corrosion resistance, an SO_2 gas test was performed based on the DIN standard DIN50018-SFW1.0S. The test conditions are listed in Table 1. This test exposes the product surface, on which condensation is formed, to SO_2 gas and is more severe than the exhaust gas environment of an actual automobile, but is used as an accelerated test for verifying the lifetime until reaching the failure mode of wire breakage due to corrosion of the product.

Figure 9 compares broken wire failure modes of the chip electrode pads and case lead frame caused by corrosion in the SO_2 gas test for a conventional product and the newly developed exhaust system pressure sensor. We verified that the newly developed exhaust system pressure sensor has more than 2.5 times that corrosion resistance of a conventional product (where 1 cycle is defined as the time from product condensation until exposure to SO_2 gas).

Table 2 Basic specifications of the exhaust system pressure sensor

Item	Units	Specification	Comments
Over-voltage	V	16.5 V	1 min
Proof Pressure	kPa abs.	600	
Storage temperature	°C	−40 to 150	
Usage temperature	°C	−40 to 135	
Power supply voltage	V	5.00±0.25	
Pressure range (absolute pressure)	kPa abs.	50 to 400	*1
Type of pressure used (gauge pressure)	kPa gauge	50 to 400	*1
Output range	V	0.5 to 4.5	
Interface	kΩ	300	Pull-up
		100	Pull-down
Diagnostic output	V	<0.2, >4.8	*2
Accuracy	%F.S.	< 1.2	10 to 85°C
	%F.S.	< 2.0	−40/135°C
Standards that have passed EMC verification		JASO D00-87, CISPR 25, ISO11452-2, ISO7637	

* 1 : Full-scale pressure can be changed freely
* 2 : Detect open mode at Vcc and/or Vout

5. Basic Specifications

Basic specifications of the newly developed exhaust system pressure sensor are as listed in Table 2. The sensor chip circuitry directly reuses a configuration

having a history of past success as a MAP sensor, and features a diagnostic function for detecting breakage of the wiring and an over-voltage protection function, and is resistant to electromagnetic noise. Either absolute pressure or gauge pressure can be selected for the pressure measurement.

6. Postscript

Fuji Electric's new exhaust system pressure sensor was developed mainly for automotive applications, but at present, efforts to reduce the exhaust gas from automobiles are targeting not only the exhaust from automobiles, but the entire process from the production to scrapping of automobiles. For example, since heavy machinery equipped with diesel engines that emit large quantities of exhaust are used in mining the iron or raw material from which automobile bodies are fabricated, and in the mining of rare metals used to make reduction catalysts and batteries, there is a movement to establish regulations for this exhaust gas and to reduce the amount of these emissions.

If the newly developed pressure sensor is to be applied to non-automotive engines, such as engines in heavy machinery and the like, then according to such conditions as the type of engine, location of sensor installation and type of fuel used, significant variations will exist in the quantity of corrosive matter contained in the exhaust gas, and in the exhaust pressure and ambient temperature, and it is important that product development be advanced with familiarity of the upper-level applications.

Fuji Electric will continue to develop world-class technology, aiming to develop products that will please our customers and contribute to environmental protection measures.

The authors wish to take this opportunity to express their gratitude to Hitachi Automotive Systems, Ltd. for their cooperation in conducting the SO_2 gas test.

References

(1) K. Saitou, Latest Trends of Automotive Sensors. CMC Publishing Co., Ltd. 2009, p.38-51.
(2) T. Takahama, et al. Semiconductor Pressure Sensors. Fuji Electric Journal. 1986, vol.59, no.11, p.707-710.
(3) K. Uematsu. About Automobile Pressure Sensors. Material Stage. Technical Information Institute, Ltd. 2009, vol.9, no.1, p.26-30.

Thermal Management Technology for IGBT Modules

Yoshitaka Nishimura † **Mitsukane Oonota** † **Fumihiko Momose** †

ABSTRACT

In power conversion systems that use IGBT modules, the thermal conductivity of the thermal grease utilized is designed as low as possible. As a result, the thermal grease thickness affects the IGBT chip temperature. This paper describes the effects of the hardness of components and the ingredients of the thermal grease on the spreading ability of the compound and the distribution of stress when tightening with screws. Additionally, in consideration of the stress distribution, we have proposed a metal mask pattern for applying the thermal grease as thinly as possible. As a result, the thermal grease can be applied at approximately 1/3rd the thickness of the conventional application technique.

1. Introduction

Recently, in response to global warming, new types of energy, such as wind and solar power, are being utilized and efforts to popularize hybrid cars are being promoted with the goal of reducing carbon dioxide emissions resulting from the use of fossil fuels. Also, as conventional electric and electronic devices are requested to provide ever higher levels of energy savings, IGBT (Insulated Gate Bipolar Transistor) modules required for power conversion and motor control are becoming more and more important. Moreover, as society becomes increasingly information-oriented, digitized data is becoming more and more prevalent, and there is renewed need for uninterruptable power supplies (UPS) and the like.

The required IGBT module characteristics differ according to the particular market, but higher efficiency and down-sizing are common requirements. For wind power generation, IGBT modules are used in the devices that convert the generated power. Power converters are often installed in limited spaces, such as inside a tower, and the IGBT modules are water-cooled to increase their mounting density and achieve a more compact size[(1)].

In response to requests for high density mounting, Fuji Electric has increased the performance[(2)] of IGBT chips. The IGBT modules have been developed with thermal management to achieve a more compact size and greater capacity simultaneously[(3),(4)]. Fuji Electric also supplies a simulator for simulating the IGBT module loss and temperature under the operating conditions, and this simulator is necessary when designing an apparatus requested by a customer.

This paper introduces technology for attaining low thermal resistance by optimizing the usage of the thermal grease that thermally connects the IGBT module and cooling fin.

2. Background

The structure of a product that uses an IGBT module and the thermal conductivities of constituent components are shown in Fig. 1. So that heat generated from the die can escape, the IGBT module is used with a cooling fin attached. The cooling fin typically used with an inverter may have a surface roughness of up to about 100 μm maximum. When an IGBT module is mounted on a cooling fin, a gap is created, and this is a factor that degrades the thermal contact resistance. Generally, in order to reduce the thermal contact resistance, thermal grease is applied (printed) between the cooling fin and IGBT module.

The thermal conductivity of a typical thermal grease is approximately 1 W/(m·K), and as can be seen in Fig. 1, thermal conductivity is lowest in the path of thermal dissipation away from the IGBT mod-

Fig.1 IGBT module structure and main thermal conductivities

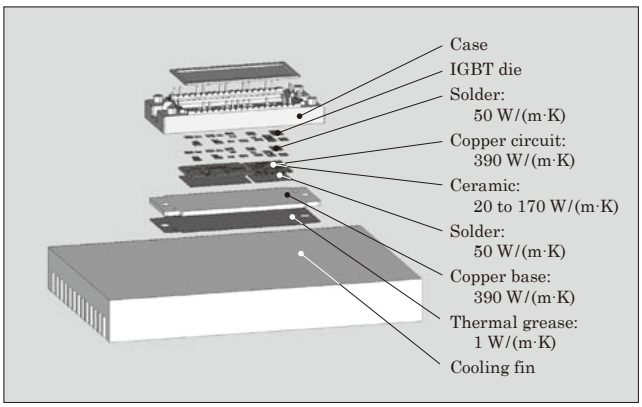

† Semiconductors Group, Fuji Electric Systems Co., Ltd.

ule. To increase the efficiency of the entire product that uses the IGBT module, reduction of the thickness of the thermal grease is requested. However, if the thickness of the thermal grease is reduced, spreading the thermal grease over the entire interface between the IGBT module and the fin will be difficult.

In the chapters below, we report on (1) factors affecting the spreadability of thermal grease and (2) the thermal grease printing method, and propose reducing the thermal contact resistance in a product that uses an IGBT module.

3. Factors Affecting the Spreadability of Thermal Grease

The thermal grease is printed onto the IGBT module or the cooling fin, and the force exerted by tightening the screws that secure the IGBT module to the cooling fin causes the thermal grease to spread out and fill the gap between the IGBT module and cooling fin. At this time, the IGBT module and cooling fin will be thermally connected. To observe the spreading of the thermal grease, grease was printed at a thickness of 30 μm in an area of 81 mm^2 between a glass block (having surface roughness of 5 μm or less) and a fin (having surface roughness of 5 μm or less), and screws to secure the glass block to the fin were tightened with 3.5 N·m of torque. The results are shown in Fig. 2. As can be seen in the figure, the thermal grease spread

Fig.2 Spreading of thermal grease

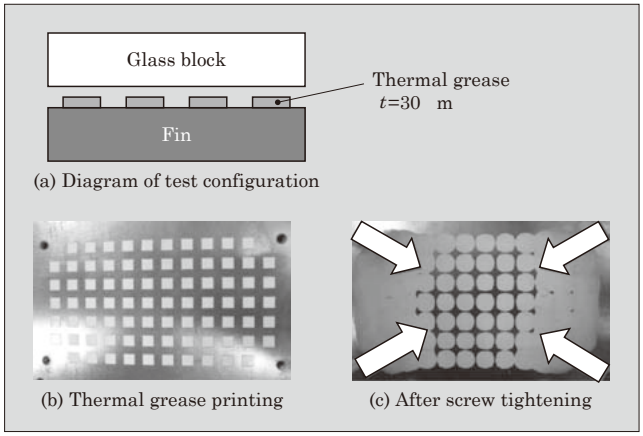

Fig.3 Results of stress distribution measurement using photoelastic camera

out around the screw locations, but despite using a flat fin, the spreading of thermal grease in the center area was poor. To investigate the cause, a photoelastic camera was used to measure the distribution of stress generated between the IGBT module and fin when the IGBT module and fin mounting screws are tightened. An FEM (finite element method) analysis was also performed at the same time.

Figure 3 shows the results of measurement with the photoelastic camera of the distribution of stress generated between the IGBT module and fin. A large stress was found to be generated in the area surrounding the screws, and this finding exhibits a similar tendency as the grease spreading test results shown in Fig. 2.

Figure 4 shows the FEM analysis model and the analysis results. The analysis was carried out for the conditions of an IGBT module size of 119 mm×59 mm and the screws being tightened with 3.5 N·m of torque. The results of the FEM analysis showed that the stress generated between the IGBT module and fin is highest at the areas around the screws, but decreases when approaching the center area. These results clearly show that generated stress between the IGBT module and fin varies according to the distance from a screw location.

Next, the relationship between stress and the thickness of the thermal grease was investigated using grease manufactured by several different companies. The following types of thermal grease were used : Electrolube's HTC, Dow Corning's SH 340, American Oil & Supply's AOS 340 and Shin-Etsu Silicone's G747. A uniform amount of each type of grease was printed onto a flat plate, and then a glass block was laid on

Fig.4 FEM analysis model and analysis results

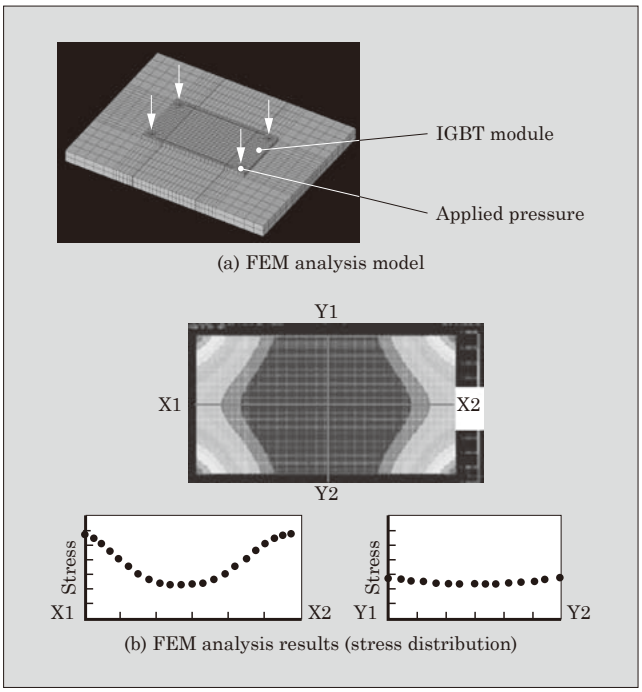

top, and pressure was applied. From the spread-out area of thermal grease at this time, the corresponding thickness of the thermal grease thickness was computed for each applied pressure.

Figure 5 shows the relationship between applied pressure and thermal grease thickness. It can be seen that the thermal grease thickness decreases as the applied pressure increases up to 0.1 MPa. However, at pressures above 0.1 MPa, the thickness did not fall below a certain level even if the applied pressure was increased. The reason for this behavior is thought to be attributable to the effect of the material composition of the thermal grease. The main components of ordinary thermal grease are ceramic powder and oil[6].

Figure 6 shows a SEM (scanning electron microscope) photograph of the ceramic particles used in thermal grease. It can be seen that the ceramic particles are several microns in size. The ceramic grains are believed to be the reason that the thermal grease thickness does not decrease below a certain level even if additional pressure is applied.

Thus, we examined factors that affect spreading of the thermal grease. As shown in Fig. 7 (a), in the case where thermal grease is present at a location of high stress in the vicinity of a screw, the gap between the module and fin will be large, and there is a concern that force may not be transmitted to the center area. In other words, the printing pattern of the thermal grease is thought to affect its spreading. Therefore, we investigated the relationship between the initial pattern and the spreading of the thermal grease. Figure 8 shows how the thermal grease spreads according to whether grease is present in the areas surrounding the screws. In the case of sample A, in which thermal grease has been printed at the screw locations, the center area does not contact the fin. However, with sample B, in which thermal grease has not been printed at the screw locations, the thermal grease spreads over the entire surface.

If there exists areas to which the thermal grease has not spread, an air layer will be formed and result in a dramatic increase in thermal resistance. Therefore, until now, poor spreading of the thermal grease was counteracted by increasing the quantity of thermal grease applied.

From the above results, it is thought that the application of thermal grease at appropriate locations will enable a smaller quantity of thermal grease to be used, resulting in a lesser thickness of the thermal grease.

Fig.5 Relationship between applied pressure and grease thickness

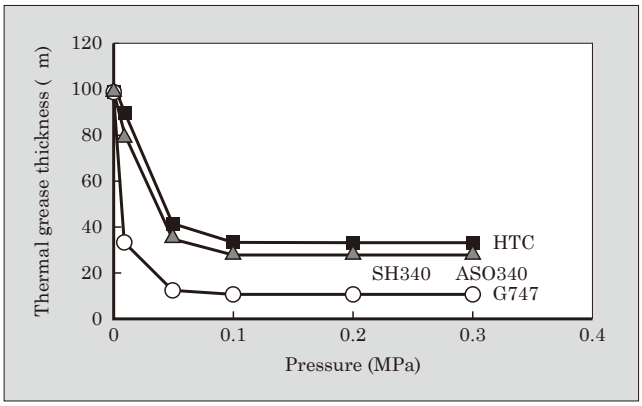

Fig.6 SEM photograph of ceramic material used in thermal grease

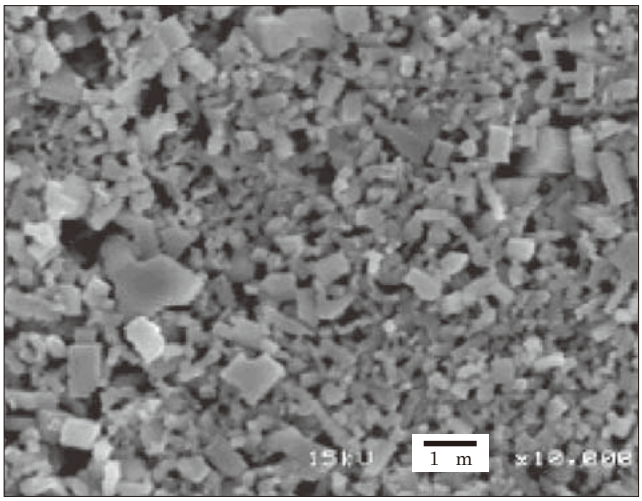

Fig.7 Relationship between grease location and pressure (schematic diagram)

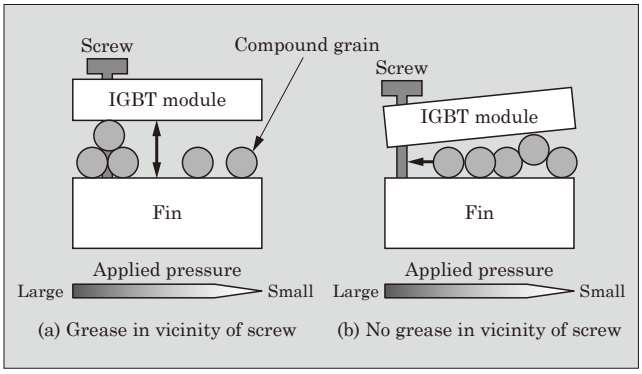

Fig.8 Relationship between thermal grease printing pattern and spreading (test results)

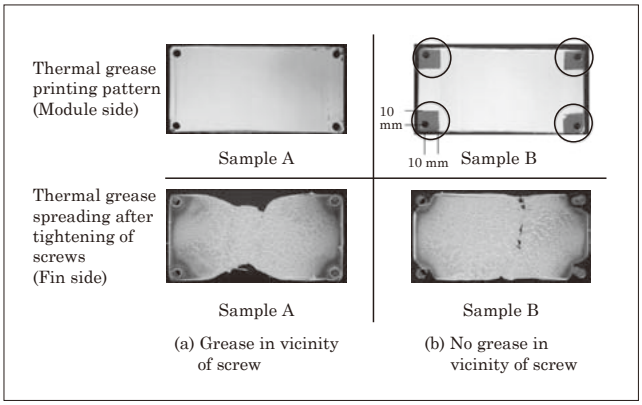

4. Development of Recommended Printing Method for Thermal Grease

4.1 Metal mask design

Based on the results of investigations into the causes of thermal grease spreading, we considered which method of thermal grease printing Fuji Electric should recommend. Typical methods of thermal grease printing involve the use of : (1) a dispenser, (2) a roller or spatula, and (3) a metal mask. When a dispenser is used for thermal grease printing, there is a large distance throughout which the grease can spread, and the spreading is easily affected by the viscosity of the thermal grease. In the case of thermal grease printing using a roller or spatula, there is significant variation in the application quantity and the quality will be inconsistent. For these reasons, Fuji Electric adopted the following method for controlling thickness of the thermal grease.

Fig.9 Thermal grease printing method using a metal mask

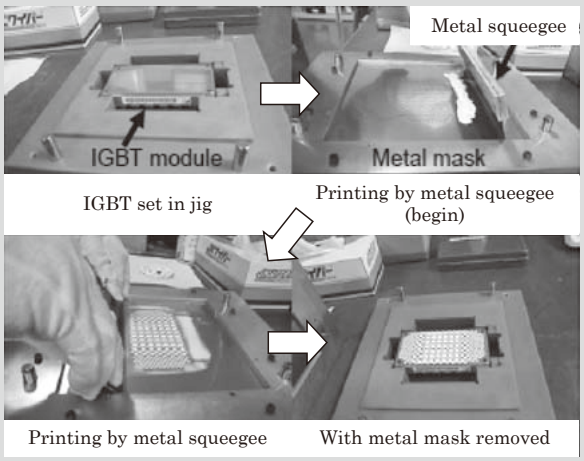

Fig.10 Recommend metal mask design

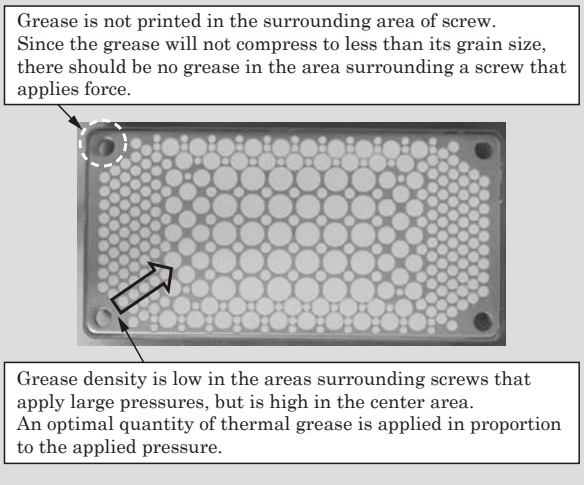

(1) Thermal grease printing shall be performed using a metal mask.
(2) Thermal grease shall be applied at appropriate locations (and no grease shall be applied in the area surrounding a screw).
(3) The quantity of grease applied shall be changed according to the level of stress generated between the IGBT module and the fin.

Figure 9 shows the method of thermal grease printing using a metal mask and Fig. 10 shows Fuji Electric's recommended metal mask design. Fuji Electric's recommended metal mask was designed so that thermal grease is not applied in the surrounding areas of screws and that the required quantity of thermal grease at each location is printed according to the stress level computed from the FEM analysis.

Next, we investigated the relationship between the printing method and the minimum thickness (printing quantity) of thermal grease required for grease spreading. For testing, a single IGBT module (having dimensions 119 mm×59 mm) and fin, and HTC thermal grease were used. Figure 11 shows the relationship between the thermal grease printing method and minimum required thickness (printing quantity). When using a roller, a mass of thermal grease corresponding to a thickness of approximately 100 μm is printed to spread over the entire surface between the IGBT module and the fin. On the other hand, it can be seen that when using Fuji Electric's recommended metal mask, a mass of thermal grease corresponding to a thickness of approximately 50 μm to spread over the entire surface between the IGBT module and the fin.

The above result demonstrates that printing using an optimal metal mask is a valid method, and that the use of Fuji Electric's recommended metal mask design

Fig.11 Relationship between thermal grease printing method and rate of spreading

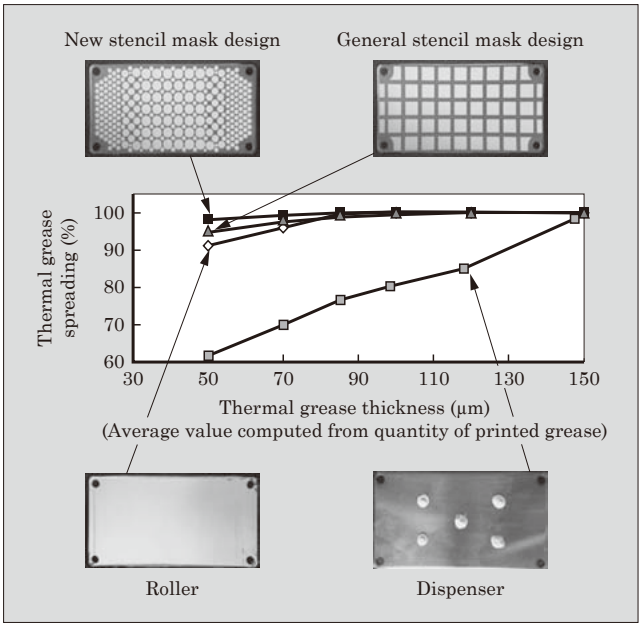

Fig.12 Relationship between thermal grease printing method and die temperature

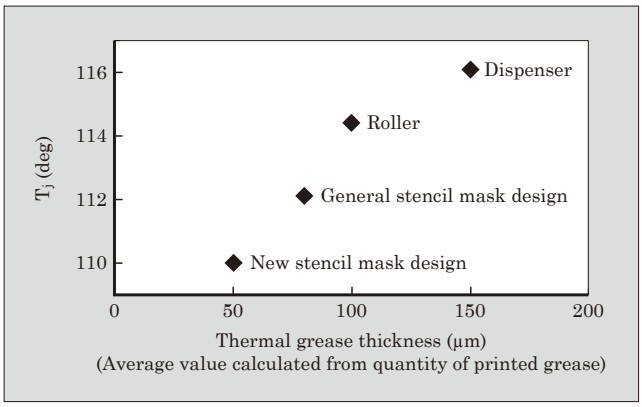

is highly effective in optimizing the quantity of thermal grease to be printed.

4.2 Affect on die temperature

We investigated the effect of the printing method on the die temperature of the IGBT module.

In the testing, using the same IGBT module and fin, a current of 80 A was applied to the IGBT die and after 5 minutes had elapsed, the die temperature was measured with an IR camera. Figure 12 shows the required minimum thermal grease thickness for each printing method, and the measured results of the IGBT die temperature for each thickness. It can be seen that the IGBT die temperatures are different according to the thermal grease printing method.

It was verified that when using Fuji Electric's recommended metal mask, the maximum IGBT die temperature was 6 °C lower than in the case of a conventional printing method. The IGBT die temperature is the largest factor affecting the lifespan and efficiency of products that utilize IGBT modules. The use of Fuji Electric's recommended metal mask enables an appropriate quantity of thermal grease to be printed and realizes a decrease in thermal resistance in products that utilize IGBT modules.

5. Postscript

The following items were clarified in the results of our study of thermal grease printing as a thermal management method in product.

(a) The stress generated between the IGBT module and fin is affected by the printed pattern of the grease.

(b) An optimal pattern and quantity exist for the thermal grease to be printed.

From the above results, an optimal metal mask design was proposed for thermal grease printing. By disclosing the thermal grease printing method to our customers and applying Fuji Electric's IGBT modules, we aim to contribute to higher efficiency and energy savings in equipment.

References

(1) Ambo, T., et al. Power Electronics for Large Scale Wind Power Generation. Journal of the Institute of Electrical Engineers of Japan. 2009, vol.129, no.5, p.291-294.

(2) Onozawa, Y. et al. Development of the Next Generation 1,200 V Trench-gate FS-IGBT Featuring Lower EMI Noise and Lower Switching Loss. ISPSD 2007, p.13-16.

(3) Kobayashi, Y. et al. New Concept IGBT-PIM Using the Latest Technology. Fuji Electric Journal. 2006, vol.79, no.5, p.358-361.

(4) Nishimura Y. et al. Development of a New-Generation RoHS IGBT Module Structure for Power Management. Transaction of the Japan Institute of Electronics Packaging. 2008, vol.1, no.1.

(5) Takaku, T. et al. Power Loss and Temperature Simulator for IGBT Module. Fuji Electric Journal. 2008, vol.81, no.6, p.438-442.

(6) Mita, K. Development of Thermal Interface Materials for IT-Related Applications (Silicone type TIM). Journal of the Society of Rubber Industry, Japan. 2005, vol.78, no.4, p.153-157.

Overseas Subsidiaries

North America

Fuji Electric Corp. of America
Sales and marketing of inverters, power distributors & control equipment, power supplies, and ring blowers

Headquarters Office
Phone +1-510-440-1060 Fax +1-510-440-1063
New Jersey Office
Phone +1-201-712-0555 Fax +1-201-368-8258
Ohio Office
Phone +1-513-326-1280 Fax +1-513-326-1288
Illinois Office
Phone +1-847-397-8030 Fax +1-847-925-9632
Virginia Office
Phone +1-540-491-9625 Fax +1-540-491-9629
Texas Office
Phone +1-713-789-8322 Fax +1-713-789-8358
Los Angeles Office
Phone +1-714-540-3854 Fax +1-714-540-5731
Marketing of semiconductor devices and photoconductive drums
Phone +1-732-560-9410 Fax +1-732-457-0042

EU

Fuji Electric Europe GmbH
Marketing of Drive & Automation equipment, semi-conductors, photoconductive drums for copiers and printers

Head Office
Phone +49-69-6690290 Fax +49-69-6661020
Erlangen Office
Phone +49-9131-729613 Fax +49-9131-28831

Fuji Electric France S.A.
Manufacture of measuring instruments
Phone +33-4-73-98-26-98 Fax +33-4-73-98-26-99

East Asia

Fuji Electric Holdings (Shanghai) Co., Ltd.
Phone +86-21-5496-3311 Fax +86-21-5496-0189

Fuji Electric Dalian Co., Ltd.
Manufacture of low-voltage circuit breakers and motors
Phone +86-411-762-2000 Fax +86-411-762-2030

Wuxi Fuji Electric FA Co., Ltd.
Manufacture of inverters
Phone +86-510-8815-2088 Fax +86-510-8815-9159

Shanghai Fuji Electric Switchgear Co., Ltd.
Manufacture of switchgear
Phone +86-21-5718-5740 Fax +86-21-5718-1448

Shanghai Fuji Electric Transformer Co., Ltd.
Manufacture and marketing of molded transformers
Phone +86-21-5718-5747 Fax +86-21-5718-5745

Shanghai General Fuji Refrigeration Equipment Co., Ltd.
Manufacture of refrigerated showcases
Phone +86-21-6921-1088 Fax +86-21-6921-1066

Fuji Electric (Shanghai) Co., Ltd.
Marketing of inverters, switchgear and transformers
Phone +86-21-5496-1177 Fax +86-21-6422-4650

Suzhou Lanlian-Fuji Instruments Co., Ltd.
Marketing of measuring instruments
Phone +86-512-8881-2966 Fax +86-512-8881-2971

Fuji Electric Technology and Service (Shenzhen) Co., Ltd.
Marketing and after-sales service of inverters
Phone +86-755-220-2745 Fax +86-755-220-5812

Hangzhou Fuji Refrigerating Machine Co., Ltd.
Development of software for vending machines and other businesses
Phone +86-571-796-8118 Fax +86-571-796-8198

Hong Kong Fujidenki Co., Ltd.
Manufacture and marketing of photoconductive drums for copiers and printers
Phone +852-2664-8699 Fax +852-2664-8040

Fuji Electric FA (Asia) Co., Ltd.
Marketing of inverters, power distributors, control equipment and semiconductors
Phone +852-2311-8282 Fax +852-2312-0566

Fuji Electric Device Technology Hong Kong Co., Limited.
Marketing of semiconductor devices
Phone +852-2311-8282 Fax +852-2312-0566

Fuji Electric Taiwan Co., Ltd.
Marketing of semiconductors
Phone +886-2-2515-1850 Fax +886-2-2515-1860

Fuji Electric FA Taiwan Co., Ltd.
Marketing of power distributors, control equipment and drive system products in Taiwan
Phone +886-2-2370-2390 Fax +886-2-2370-2389

Atai Fuji Electric Co., Ltd.
Manufacture of small- to medium-capacity industrial motors
Phone +886-3-321-3030 Fax +886-3-321-7890

Fuji Electric FA Korea Co., Ltd.
Materials procurement and marketing of electrical and electronic machinery and components
Phone +82-2-780-5011 Fax +82-2-783-1707

Korea FA Systems Co., Ltd.
Development and marketing of software for computers
Phone +82-2-598-0651 Fax +82-2-573-1904

Southeast and South Asia

Mahajak International Electric Co., Ltd.
Manufacture and marketing of watt-hour meters
Phone +66-2-253-2350 Fax +66-2-253-2354

Fuji Electric (Malaysia) Sdn. Bhd.
Manufacture of magnetic recording media
Phone +60-4-403-1111 Fax +60-4-403-1491

Fuji Electric Semiconductor (Malaysia) Sdn. Bhd.
Manufacture of power semiconductors
Phone +60-4-403-1111 Fax +60-4-403-5993

Fuji Electric Philippines, Inc.
Manufacture of power semiconductors
Phone +63-2-844-6183 Fax +63-2-844-6196

Fuji-Haya Electric Corp. of the Philippines
Manufacture and marketing of switch boards and electrical control equipment
Phone +63-2-892-8886 Fax +63-2-893-5645

P.T. Fuji Dharma Electric.
Manufacture of watt-hour meters
Phone. +62-21-4606247 Fax +62-21-4610338

Fuji Electric Asia Pacific Pte. Ltd.
Marketing of Drive & Automation equipment and semiconductors, in Southeast Asia
Phone +65-6533-0010 Fax +65-6533-0021

Printed on recycled paper